ANALYSIS OF ADDITIVELY MANUFACTURED 17-4PH STAINLESS STEEL

ANALYSIS OF ADDITIVELY MANUFACTURED 17-4PH STAINLESS STEEL

By SIMON COULSON, B.Eng.

A Thesis Submitted to the School of Graduate Studies in Partial Fulfilment of the Requirements for the Degree Master of Applied Science

McMaster University MASTER OF APPLIED SCIENCE (2018) Hamilton, Ontario (Materials Science and Engineering)

TITLE: Analysis of Additively Manufactured 17-4PH Stainless Steel

AUTHOR: Simon Coulson B.Eng. (McMaster University)

SUPERVISOR: Professor Hatem Zurob

NUMBER OF PAGES: xiv, 52

Lay Abstract

17-4PH stainless steel is a martensitic alloy, that can be precipitation hardened when used in traditional manufacturing processes. Within a selective laser melting process, it will exhibit up to 50% lower yield strength and 600% higher elongation. This behaviour is caused by retained austenite, which is stabilized by the introduction of nitrogen during the powder atomization process. As a result, the alloy exhibits transformation induced plasticity. Existing literature states the alloy's microstructure can be controlled by altering the selective laser melting process atmosphere or using heat treatment to achieve traditional mechanical properties. However, the production and preparation of samples generates a surface transformation which was misinterpreted as a complete bulk transformation. Therefore, the change in microstructure from altering the process atmosphere is only detectable through surface analytical techniques. It is proposed that the rapid cooling rates of SLM form a non-equilibrium state, keeping nitrogen in solution. Subsequent heat treatment allows the formation of nitrides resulting in the Ms being brought above room temperature.

Abstract

Selective laser melting of nitrogen gas atomized 17-4PH stainless results in up to 50% lower yield strength and 600% higher elongation compared to traditionally processed, wrought 17-4PH. This drastic difference in mechanical properties is commonly attributed to the presence of high volume fractions of retained austenite within the as-built microstructure. The factors leading to the increased level of retained austenite have not been clarified in the literature. Furthermore, the amount of retained austenite reported within published literature vary widely, even with the use of identical process parameters. Manufacturers of selective laser melting systems state that solution annealing and precipitation hardening will achieve traditional mechanical properties, thereby removing all retained austenite. Once again, it is not clear, how the recommended solution and precipitation treatments lead to the desired changes in microstructure.

The research within this thesis establishes that there is up to 0.12wt% higher nitrogen content within additively manufactured 17-4PH, compared to traditionally manufactured 17-4PH, as a result of the powder atomization process. The increased nitrogen is able to stabilize the austenitic phase by reducing the Ms temperature below ambient temperatures. Fertiscope bulk phase analysis demonstrates that the processing atmosphere during selective laser melting cannot alter the fraction of retained austenite in the as-built material. The depression of the Ms temperature in the printed parts is confirmed by dilatometry.

Due to the TRIP phenomenon, during sample preparation, it was found that the austenite would transform to 80% martensite at the surface. This transformation will greatly impact the phases detected when x-ray diffraction is used for analysis, leading to a wide variety of reported retained austenite values within literature.

A mechanism based on the precipitation of nitrides during solution-treatment has been proposed to explain how heat-treatment of the printed parts can lead to a martensitic microstructure with comparable mechanical properties to those of wrought alloys.

Acknowledgements

I would first like to thank my supervisor, Professor Hatem Zurob, whose immense knowledge, support, and flexibility allowed me to undertake this challenge later in my career.

Additionally, I would like to thank Mohawk College of Applied Arts and Technology for providing the opportunity and assistance to pursue this accomplishment. The terrific staff at McMaster University for their help in sample preparation and analysis; Hamid Aziz, Douglas Culley, Victoria Jarvis, and Chris Butcher. The Thermal Management Research Laboratory, Ahmed Ali Mahmoud, Ryan Rogers, and Michael Cino for their assistance in the powder analysis. Marta Aniolek of CanmetMATERIALS for supporting dilatometry analysis.

Finally, I would like to thank my loving family. My wife Jennifer, who encouraged me to further my education fully knowing the amount of proof reading she would be required to do! Our daughter Claire who was always included in my presentations, our son Zachary who was born half way through my studies, and our dog Halle for always informing me when someone was at the door, regardless if they were knocking or walking past.

Table of Contents

Lay Abstract ***ii***

Abstract ***iii***

Acknowledgements ***v***

Table of Contents ***vi***

List of Figures ***x***

List of Tables ***xii***

List of all Abbreviations and Symbols ***xiii***

1. Introduction ***1***

2. Literature Review ***2***

2.1 Selective Laser Melting **2**

2.1.1 SLM Process Parameters 2

2.1.2 SLM Process Operation 4

2.1.3 Powder Production 5

2.2 Comparison of Mechanical Properties **6**

2.3 Existing Research **6**

2.3.1 Retained Austenite within Existing Research 7

2.3.2 Possible Factors that Influence the Amount of Retained Austenite 9

2.4 Summary **10**

3. Experimental Methods ***11***

3.1 Sample Preparation: **11**

3.1.1 Additive Manufacturing 12

3.1.2 Traditional Manufacturing 12

3.2 Thermal and Mechanical Treatments **13**

3.3 Mounting and Polishing **14**

3.4 Sample Notation **14**

3.5 Analytical Techniques **15**

3.5.1 Chemical Analysis 16

3.5.2 Nitrogen Analysis 16

3.5.3 Particle Size, Distribution, and Shape 16

3.5.4 Retained Austenite 17

3.5.5 Grain Structure 18

3.5.6 Dilatometry 18

4. Experimental Results ***19***

4.1. Chemical Analysis **19**

4.2 Nitrogen Analysis **20**

4.3 Particle Size, Distribution, and Shape **20**

4.4 Retained Austenite **22**

4.5 Grain Structure **24**

4.6 Dilatometry **25**

4.7 Summary **27**

5 Discussion ***29***

5.1 Influence of Process Atmosphere on Retained Austenite **29**

5.2 Influence of Nitrogen on Retained Austenite **30**

5.2.1 Origin of Nitrogen Content 31

5.2.2 Effect of Nitrogen on the Ms Temperature 31

5.2.3 Nitrogen Stability within the Alloy 32

5.2.4 Diffusion of Nitrogen 33

5.2.5 Summary 34

5.3 Influence of Deformation on Retained Austenite **35**

5.3.1 Applied Deformation 35

5.3.2 Unintentional Deformation 35

5.3.3 Summary 36

5.4 Manufacturers Datasheets **37**

5.4.1 EOS StainlessSteel GP1 37

5.4.2 EOS StainlessSteel 17-4PH 38

5.4.3 EOS StainlessSteel 17-4PH IndustryLine 38

5.4.4 Summary 39

6 Conclusion ***41***

6.2 Future Work **42**

References ***44***

Appendix A ***50***

Appendix B ***52***

List of Figures

Figure 1: Illustration of SLM parameters (Yap et al. 2015) 3

Figure 2: Illustration of SLM system components (Additively AG 2018) 4

Figure 3: Illustration of gas atomization process (LPW Technology Ltd. 2018) 5

Figure 4: Retained austenite within all published literature that studied influence of the SLM process on 17-4PH 7

Figure 5: Retained austenite within published literature after refinement to a common set of process parameters 8

Figure 6: Schematic of tube sample used for dilatometry analysis 11

Figure 7: Particle size distribution 17-4PH powder, according to ASTM B822, reveals 50% of the particles have a diameter less 34μm, while 90% are less than 58μm 21

Figure 8: Optical images of 17-4PH powder demonstrating the consistency of particle size and shape 21

Figure 9: SEM images of 17-4PH powder demonstrating highly spherical particles with uniform surface morphology. 22

Figure 10: EBSD band contrast of AM samples produced under nitrogen after a) polishing showing a mix of large and fine grains b) solution annealing at 1040°C and polishing showing fine grains associated with a martensitic structure 24

Figure 12: EBSD band contrast of AM samples produced under argon after a) polishing showing a mix of large and fine grains 25

Figure 14: Dilatometry of reference sample exhibiting volume increase associated with a martensitic transformation upon cooling 26

Figure 15: Dilatometry of AM sample produced in nitrogen atmosphere does not exhibit a volume increase associated with a martensitic transformation upon cooling 26

Figure 16: Dilatometry of AM sample produced in argon atmosphere does not exhibit a volume increase associated with a martensitic formation upon cooling 27

Figure 17: Phase Diagram of 17-4PH at 1atm pressure illustrating the stability of nitrogen in solution 32

Figure 18: Average nitrogen content over time due of a 5mm thick cylinder with a nitrogen concentration of 0.14wt% within the bulk and 0.00wt% at the surface. A diffusion coefficient of 1.84x10-11m^2/s at 1040°C was assumed for calculation. 33

Figure 19: Nitrogen concentration profile of a 5mm sample after solution annealing at 1040°C for 30minutes. 34

Figure 20: Additive manufacturing software parameters - strips 50

Figure 21: Additive manufacturing software parameters - up/down skin 50

List of Tables

Table 1: Comparison of 17-4PH mechanical properties for typically values of traditionally manufactured alloy in as-received state and additively manufactured alloy in as-built state. 6

Table 2: Most common additive manufacturing process parameters used for the production of nitrogen atomized 17-4PH powder within published literature 8

Table 3: Additive manufacturing process parameters used to create samples for testing based on most commonly occurring values within literature review 12

Table 4: Production process for tube samples used within dilatometry 13

Table 5: Production process for disk samples used within remaining testing 13

Table 6: Notation of all sample conditions produced for testing and analysis 15

Table 7: ASTM composition specifications and measured compositions of wrought and printed specimens in wt%. The accuracy of the measured compositions is estimated at ± 2% of the measured concentration in the case of the substitutional elements. In the case of carbon and sulfur the values are within +/- 0.005 wt%. 19

Table 8: Measured nitrogen content (wt%), of reference wrought 17-4PH material as well as AM powder and AM components manufactured and heat-treated under different conditions. The accuracy of the measurements is ± 0.01wt% 20

Table 9: Results of retained austenite volume fraction for fertiscope (±0.2%), XRD (±3%), and EBSD. Error of EBSD cannot be accurately measured but will be within ±3% based on image analysis. 24

Table 10: Additive manufacturing parameters used in this study. 51

Table 11: Polishing parameters 52

List of all Abbreviations and Symbols

3D	Three Dimensional
17-4PH	17-4 Precipitation Hardenable Stainless Steel
17-4PH Powder	Raw powder feedstock for SLM process
Ac1 & Ac3	Austenite transition temperatures
AM	Additive Manufacturing
AM-Ar	Additively Manufactured under Ar atmosphere in as-built condition
AM-Ar+LN2	Additively Manufactured under Ar atmosphere + cryogenic treatment
AM-Ar-P	Additively Manufactured under Ar atmosphere, mounted and polished
AM-Ar+R#	Additively Manufactured under Ar atmosphere + rolling treatment where # is the percentage reduction of thickness
AM-Ar+SA	Additively Manufactured under Ar atmosphere + solution annealing heat treatment
AM-Ar+SA-P	Additively Manufactured under Ar atmosphere + solution annealing heat treatment, mounted and polished
AM-Ar+SA+H900	Additively Manufactured under Ar atmosphere + solution annealing heat treatment in + precipitation hardening
AM-N2	Additively Manufactured under N2 atmosphere in as-built condition
AM-N2+LN2	Additively Manufactured under N2 atmosphere + cryogenic treatment
AM-N2-P	Additively Manufactured under N2 atmosphere, mounted and polished
AM-N2+R#	Additively Manufactured under N2 atmosphere + rolling treatment where # is the percentage reduction of thickness

AM-N2+SA	Additively Manufactured under N2 atmosphere + solution annealing heat treatment
AM-N2+SA-P	Additively Manufactured under N2 atmosphere + solution annealing heat treatment, mounted and polished
AM-N2+SA+H900	Additively Manufactured under N2 atmosphere + solution annealing heat treatment + precipitation hardening
ASTM	American Society for Testing and Materials
DMLS	Direct Metal Laser Sintering
EOS	EOS GmbH Electro Optical Systems
H900	ASTM specified precipitation hardening method
M280	EOS M280 DMLS system
Ms	Austenite to Martensite formation
Reference	Traditionally Manufactured
Reference+SA	Traditionally Manufactured + solution annealing heat treatment
SA	Solution Annealing
SEM	Scanning Electron Microscope
SLM	Selective Laser Melting
TM	Traditional Manufacturing
TRIP	Transformation Induced Plasticity

1. Introduction

Three Dimensional (3D) printing was initially developed in 1987 (Wohlers and Gornet 2014) by utilizing photopolymerized resins to create objects layer-by-layer from 3D computer aided design. Due to the limited availability of materials, process reliability, and cost, it was primarily used for prototype production. In the subsequent three decades, significant advancements have been made by the introduction of new 3D printing methods, materials, and reliability, allowing 3D printing to be utilized for the production of end use components. To dissociate the decades old stereotype that 3D printing was for prototypes, a new term was coined, Additive Manufacturing (AM). The thought being that the AM process should be viewed as just another manufacturing process with its own set of design guidelines.

One key factor that is slowing the adoption of AM, is that the resulting mechanical properties are different from their traditionally manufactured counterparts. Objects produced via AM exhibit anisotropy, due to the layer-by-layer construction process, with their yield strength, young's modulus, and hardness frequently being 5-10% lower than those of Traditional Manufactured (TM) counterparts. Subsequent post processing can be performed to achieve near equivalent properties in most cases. One notable exception is 17-4PH Stainless Steel (17-4PH), which is a martensitic precipitation hardening alloy when produced by traditional manufacturing methods. Within the AM process known as Selective Laser Melting (SLM), 17-4PH exhibits up to 50% lower yield strength and 600% higher elongation than its wrought counterpart.

The research within this thesis will focus on evaluating these unique mechanical properties, how the SLM process alters them, and if this effect can be controlled.

2. Literature Review

To start, a general introduction to the process of selective laser melting is presented in section 2.1, followed by a comparison of TM and AM mechanical properties. In section 2.2 a review of existing literature reveals retained austenite is responsible for the variation in mechanical properties. Finally, in section 2.3, further examination was done into the volume fractions of retain austenite and formation theories within existing literature.

2.1 Selective Laser Melting

The American Society for Testing and Materials (ASTM) defines powder bed fusion as "an additive manufacturing process in which thermal energy selectively fuses regions of a powder bed." (ASTM International 2012). A subcategory, laser sintering, is the most commonly used and denotes the thermal energy source as a laser. Within industry, laser sintering is often referred to as Direct Metal Laser Sintering (DMLS), trademarked by EOS GmbH Electro Optical Systems (EOS) to designate their equipment, or SLM which is used generically for equipment by any manufacturer. Although the terms of fusion, sintering, and melting are used interchangeably within industry and literature; in all scenarios the material is fully melted to achieve near fully dense parts, therefore the term SLM will be used within the context of this research.

2.1.1 SLM Process Parameters

The process of SLM has controllable parameters, however, the most critical parameters are laser power, laser speed, hatching, layer thickness, and process atmosphere, which are illustrated in Figure 1.

The laser power is expressed in watts and is the measurement of power delivered to the power bed, in joules per second, and not the power of the laser utilized. The laser speed, sometimes referred to as scanning speed, is expressed in mm/s and controlled by the actuation of the optics system. The hatching spacing, also referred to the hatching distance or simply hatching, is the centre to centre distance between subsequent laser passes and expressed in microns. The layer thickness is controlled by the movement of the powder bed, expressed in microns, and the distribution of additional powder afterwards. Finally, the process atmosphere is controlled by the supplied gases, with nitrogen typically being utilized for non-reactive materials and argon for reactive materials

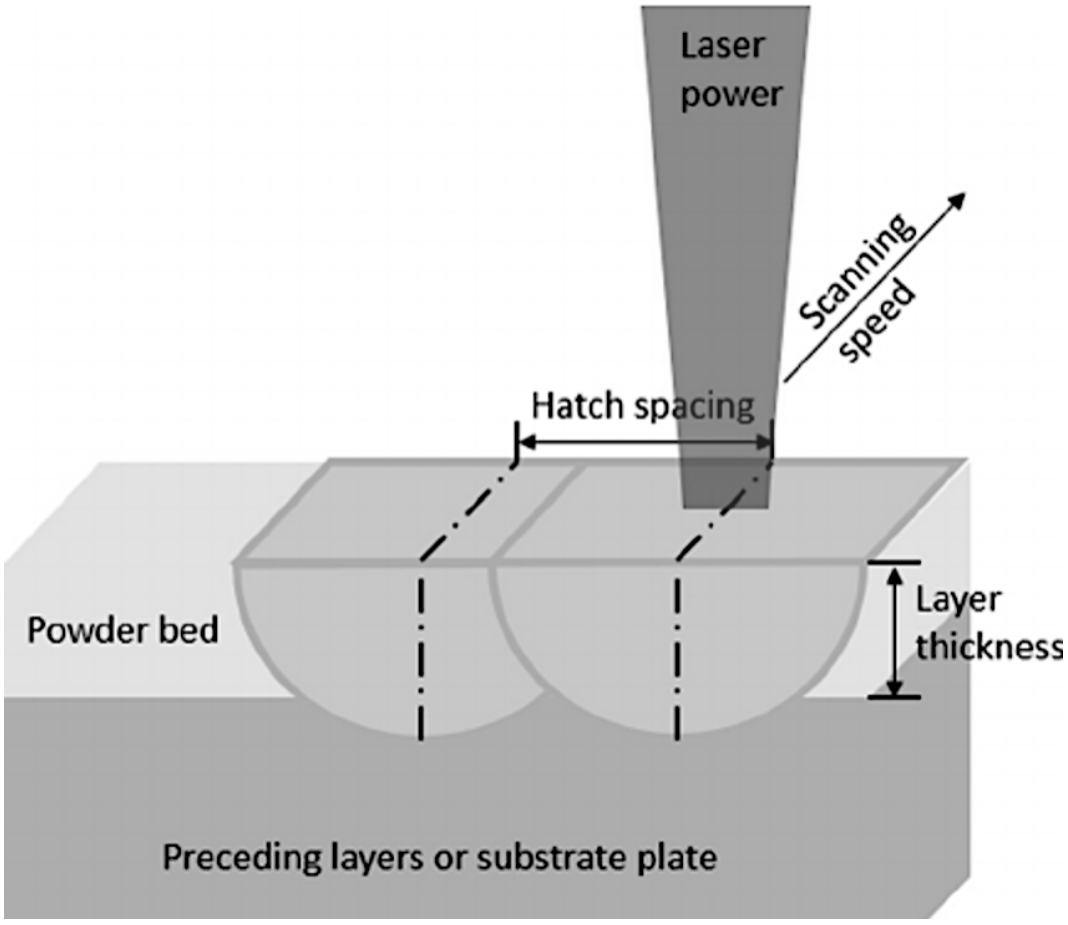

Figure 1: Illustration of SLM parameters (Yap et al. 2015)

2.1.2 SLM Process Operation

The process operation is illustrated in Figure 2 and carried out in the following order. First, the metal powder supply is raised up while the build platform is lowered by the defined layer thickness. The recoat arm will then spread the metal powder from the supply across the build platform. The laser is then activated with the predefined laser power, with the X-Y scanning mirror controlling the laser speed and hatch spacing. Once laser scanning is complete, the recoat arm will return to its initial position and the process will be repeated until the component is complete. Initial layers will deposit the material directly on the build plate, sometimes referred to as the substrate plate, with all subsequent layers building upon the surface area of the previous layers. If the component does not have sufficient surface area to build on, a support structure will be added to the design. A support structure is another component that is produced with intentional porosity to allow for easier removal during post processing. Once the SLM process is complete, the part will need to be separated from the build platform through manual or automated machining processes.

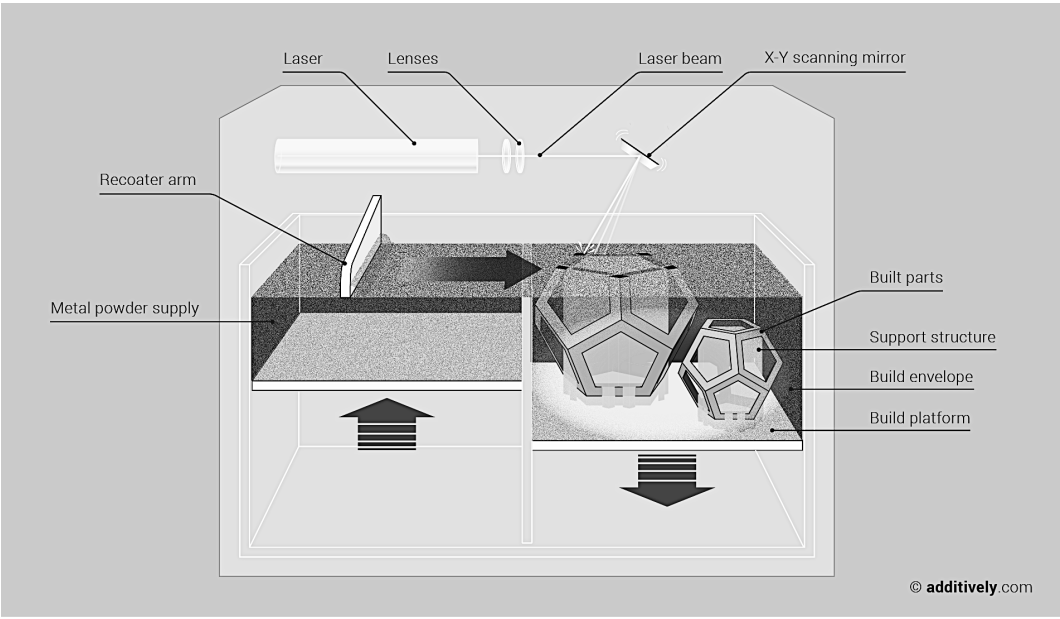

Figure 2: Illustration of SLM system components (Additively AG 2018)

2.1.3 Powder Production

The powder used in a SLM process can be produced by a variety of methods, however, several considerations must be taken into account to avoid defects within the resulting material. With the intent of creating a powder bed with the highest packing density possible, the powder used needs to have uniform particle shape (Cooke and Slotwinski 2015), size and distribution (Sutton et al. 2017), and no agglomerate (Simchi 2004). Gas atomization can produce powders of reactive materials by utilizing argon. Nitrogen is used for producing unreactive materials. The process provides a cost effective combination of the previously discussed powder characteristics (Dawes and Bowerman 2015) and is most commonly used in the industry. The gas atomization process is illustrated in Figure 3. The alloy is melted and directed through a nozzle where jet(s) direct the gases, at high velocity and pressure, at the molten material (Fritsching and Uhlenwinkel 2012). This impinges the molten material upon exiting the nozzle, breaking it up into spherical particles.

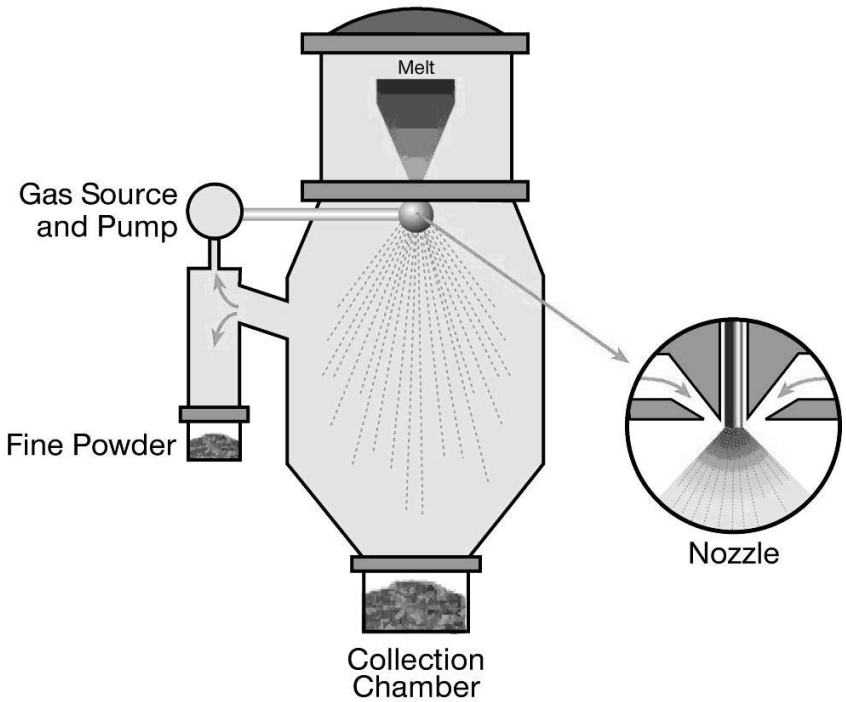

Figure 3: Illustration of gas atomization process (LPW Technology Ltd. 2018)

2.2 Comparison of Mechanical Properties

Additively manufactured 17-4PH exhibits vastly different mechanical properties compared to its traditionally manufactured counterpart. Table 1 was compiled using datasheets supplied by ASTM (ASTM International 2010) and AK Steel (AK Steel Corporation 2007) for the typical values of the TM alloy in its as-received state. The AM values were compiled using datasheets supplied by EOS (EOS GmbH - Electro Optical Systems 2009, 2015) in their as-built state.

	Tensile (MPa)	**Yield (MPa)**	**Elongation (.2%)**	**Hardness (HRC)**
TM	1103	1000	5	38
AM (XY/Z)	930/960	645/630	31/35	23

Table 1: Comparison of 17-4PH mechanical properties for typically values of traditionally manufactured alloy in as-received state and additively manufactured alloy in as-built state.

2.3 Existing Research

It is well established that components produced with SLM will have mechanical properties that vary from their traditionally manufactured counterparts. This is attributed to the layer-by-layer production process of AM resulting in finer and, often, elongated grains (Shellabear and Nyrhilä 2004). However, 17-4PH demonstrates such drastically different mechanical properties compared to those of wrought 17-4PH. This difference cannot be solely attributed to the grain-refinement during the AM process. EOS elaborated that these differences were caused "…by the formation of a duplex-type steel structure with interlocked phases of austenite and martensite/deltaferrite during the extremely rapid melting and re-solidification" (Shellabear and Nyrhilä 2007). The presence of

a high volume fraction of retained austenite within this martensitic alloy would qualitatively rationalize the significant difference in the resulting mechanical properties.

2.3.1 Retained Austenite within Existing Research

EOS does not provide details regarding the amount of retained austenite in specimens produced by SLM using the powders and process parameters supplied by the company. A meta-analysis (n=13) was performed on all literature that studied the influence of the SLM process on 17-4PH since the introduction of "EOS StainlessSteel GP1" in 2007, and the completion of this literature review, 2017. The results are presented in Figure 4. The results show no definitive trends. Given the large number of parameters within the AM process, the meta-analysis was further refined (n=3) to a common set of process parameters defined in Table 2, with the results presented in Figure 5.

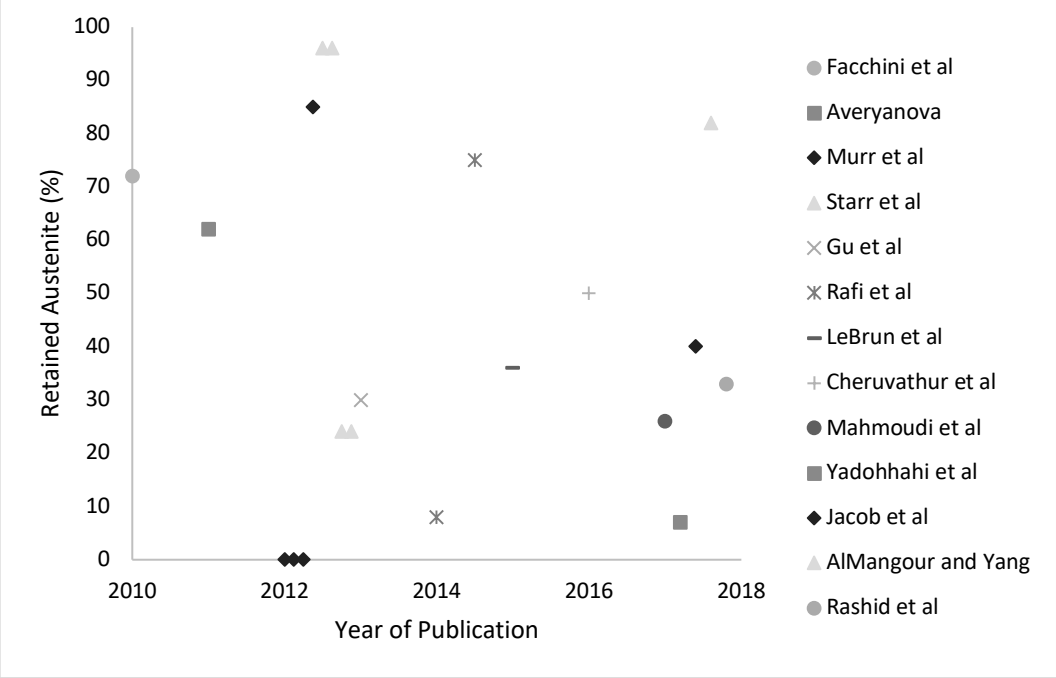

Figure 4: Retained austenite within all published literature that studied influence of the SLM process on 17-4PH

Material	Nitrogen atomized 17-4PH stainless steel
System	EOS M270/M280
Laser Power (W)	195 ± 5
Laser Speed (mm/s)	900 ± 100
Hatching (μm)	100 ± 10
Layer Thickness (μm)	40
Process Atmosphere	nitrogen or argon

Table 2: Most common additive manufacturing process parameters used for the production of nitrogen atomized 17-4PH powder within published literature

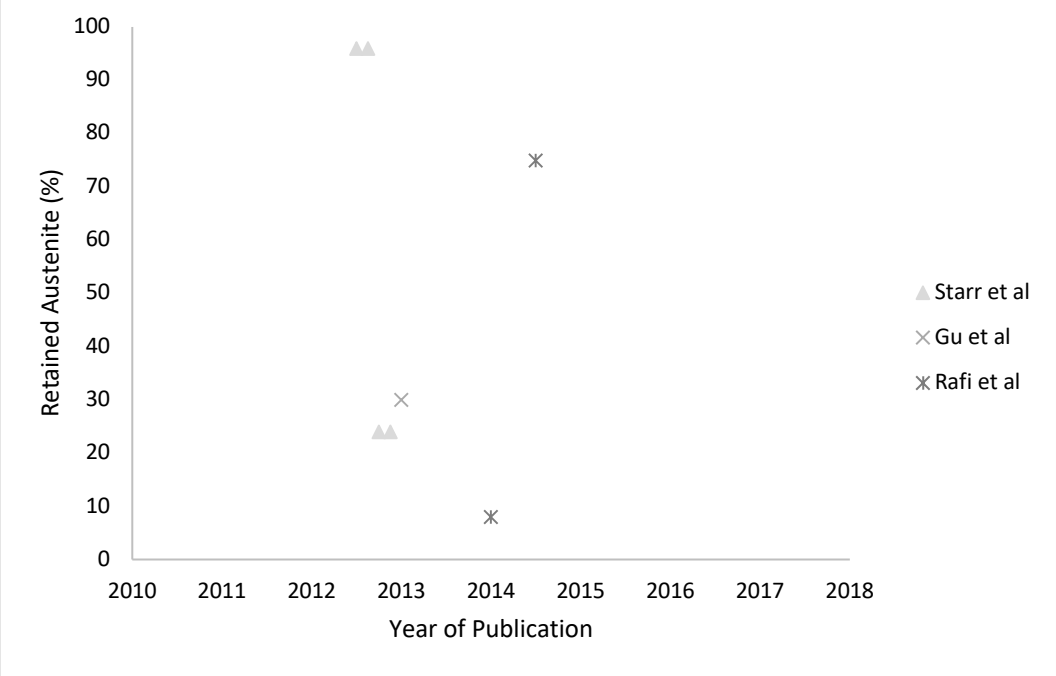

Figure 5: Retained austenite within published literature after refinement to a common set of process parameters

With this further refinement there was still no clear indication of the amount of retained austenite in the as-built 17-4PH samples. Several arguments have been put forward in the literature regarding the retention of austenite in parts prepared by SLM. These arguments are reviewed next.

2.3.2 Possible Factors that Influence the Amount of Retained Austenite

AlMangour and Yang argued that the rapid cooling rates of the SLM process results in the formation of fine grains, thereby reducing the Austenite to Martensite formation (Ms) temperature (AlMangour and Yang 2017). The presence of a high nitrogen content, within the powders obtained by gas atomization, further reduces the Ms temperature (Rafi et al. 2014). As a result, a significant volume fraction of retained austenite can exist in the as-built material at room temperature. The retained austenite, however, is metastable, and transforms to martensite during deformation (Facchini et al. 2010). This introduces an additional complication with respect to measurement of retained austenite fractions because some sample preparation methods may lead to local deformation and martensite formation at the surface.

Some authors reported that the high volume fraction of retained austenite in the as built part could be reduced by reheating the material above its austenite transition temperature and subsequent cooling to room temperature. This heat-treatment was experimentally shown to transform most of the austenite to martensite (Starr et al. 2012). No arguments were offered to explain why the reheating step made it possible for the martensite to form during cooling.

Gu et al. argued that the amount of retained austenite will not be influenced by varying laser power and speed (Gu et al. 2013). Murr et al. argued that by using an argon atmosphere, instead of the recommended nitrogen atmosphere, a reduced cooling rate would be obtained due to argon's lower thermal conductivity and this would lead to the formation of a martensitic microstructure (Murr et al. 2012). This however is contrary to general wisdom in which faster cooling rates will result in greater martensite formation.

2.4 Summary

The bulk of existing literature shows that retained austenite is present within the as built AM 17-4PH material. Verification is needed to determine if it is indeed possible to control the resulting microstructure within the AM process, what is causing the formation of retained austenite, and why there is such a wide range of retained austenite volume fractions in published literature. In the following section, a series of experiments will be proposed to clarify these issues.

3. Experimental Methods

A series of experiments were designed to clarify if the AM process parameters can control the resulting microstructure, what is causing the formation of retained austenite, and why there is such a wide range of retained austenite volume fractions in published literature. To start, sample preparation is described in section 3.1. This is followed by a series of thermal and mechanical treatments that have been reported, or suspected, to be capable of causing a reduction in austenite are outlined in section 3.2. The mounting and polishing process is subsequently outline in section 3.3. The resulting samples, and notation, are outlined in section 3.4, with the methods of analysis being described in section 3.5.

3.1 Sample Preparation:

The majority of testing was carried out on desk specimens with a diameter of 15 mm and a thickness of 3 mm. The only exception was the dilatometer testing; a tube was utilized to allow for high cooling rates without deformation using the dimensions defined in Figure 6.

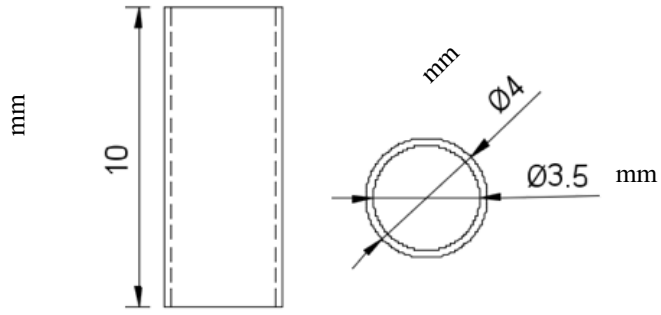

Figure 6: Schematic of tube sample used for dilatometry analysis

3.1.1 Additive Manufacturing

All additively manufactured samples were produced utilizing an EOS M280 DMLS system (M280) and nitrogen gas atomized "EOS Stainless Steel GP1" powder purchased directly from EOS. Two batches of samples were produced using the parameters in Table 5, with only the atmosphere being varied. Within each batch, both the tube and disk samples were produced simultaneously. A 5mm support structure was added to the base of the samples to adhere to a 304L stainless steel build plate. Samples were removed from the build plate using a Baxter Verticut 115C bandsaw, under coolant, with remaining support being removed via a hand file. *Additional details in Appendix A.*

Batch	**1**	**2**
Atmosphere	nitrogen	argon
Layer Thickness (um)	40	
Power (W)	195	
Speed (mm/s)	900	
Hatching (mm)	0.1	

Table 3: Additive manufacturing process parameters used to create samples for testing based on most commonly occurring values within literature review

3.1.2 Traditional Manufacturing

In order to benchmark the results, a group of traditionally produced specimens of 17-4PH were machined. All traditionally manufactured samples were produced from a wrought 25.4mm diameter bar of 17-4PH stainless steel purchased from the Metal Supermarkets IP Inc. Both disk and tube samples were machined with the same dimensions described above. Given the potential for machining to deform the surface and change the amount of retained austenite, the detailed machining steps are provided in Table 3, for tube specimens and Table 4, for disk specimens.

Step	Operation
1	Outer diameter turned down to 4mm
2	Inner diameter bored out to 3.5mm
3	Length parted off at 10mm

Table 4: Production process for tube samples used within dilatometry

Step	Operation
1	Outer diameter turned down to 15mm
2	Length parted off at 3mm

Table 5: Production process for disk samples used within remaining testing

3.2 Thermal and Mechanical Treatments

Various thermal treatments were performed in order to understand the microstructure evolution of the material. Solution Annealing (SA) was performed on a subset of samples according to ASTM A564 -13 (ASTM International 2010), which consists of holding at 1040°C for 30 minutes then air cooling below 32°C by removing samples from furnace. Precipitation hardening heat-treatment (H900) was performed on a subset of samples according to ASTM A564 -13 (ASTM International 2010). This heat-treatment consists of holding at 480°C for 1 hour, followed by air cooling by removing samples from furnace. Cryogenic treatment (LN2) was performed on a subset of samples by submerging them in liquid nitrogen for 45 minutes.

A subset of samples was rolled to thickness reductions of 10%, 30%, and 50% using a benchtop rolling mill. Deformation was applied with a 5% reduction per pass.

3.3 Mounting and Polishing

Samples for optical metallography and SEM were hot-mounted in bakelite and automatically polished using a Struers Tegramin-25 polishing machine. Given the potential for the transformation of retained austenite to martensite during polishing, the polishing steps were carefully controlled to minimize variability between samples and to reduce martensite formation during polishing. Complete details of the polishing procedure used are provided in Appendix B.

3.4 Sample Notation

The sample production conditions and subsequent preparation methods are outline in Table 6, with the associated notation that will be used throughout the course of this research.

Notation	**Condition**
Reference	Traditionally Manufactured
Reference+SA	Traditionally Manufactured + solution annealing heat treatment
17-4PH Powder	Raw powder feedstock for SLM process
AM-N2	Additively Manufactured under N2 atmosphere in as-built condition
AM-N2-P	Additively Manufactured under N2 atmosphere, mounted and polished
AM-N2+SA	Additively Manufactured under N2 atmosphere + solution annealing heat treatment
AM-N2+SA-P	Additively Manufactured under N2 atmosphere + solution annealing heat treatment, mounted and polished

AM-N2+SA+H900	Additively Manufactured under N2 atmosphere + solution annealing heat treatment + precipitation hardening
AM-N2+LN2	Additively Manufactured under N2 atmosphere + cryogenic treatment
AM-N2+R#	Additively Manufactured under N2 atmosphere + rolling treatment where # is the percentage reduction thickness
AM-Ar	Additively Manufactured under Ar atmosphere in as-built condition
AM-Ar-P	Additively Manufactured under Ar atmosphere, mounted and polished
AM-Ar+SA	Additively Manufactured under Ar atmosphere + solution annealing heat treatment
AM-Ar+SA-P	Additively Manufactured under Ar atmosphere + solution annealing heat treatment, mounted and polished
AM-AR+SA+H900	Additively Manufactured under Ar atmosphere + solution annealing heat treatment in + precipitation hardening
AM-Ar+LN2	Additively Manufactured under Ar atmosphere + cryogenic treatment
AM-Ar+R#	Additively Manufactured under Ar atmosphere + rolling treatment where # is the percentage reduction thickness

Table 6: Notation of all sample conditions produced for testing and analysis

3.5 Analytical Techniques

A series of analytical techniques were selected to clarify if the AM process parameters can control the resulting microstructure, what is causing the formation of retained austenite, and why there is such a wide range of retained austenite volume fractions in published literature.

3.5.1 Chemical Analysis

The chemical compositions of the materials were first characterized to determine conformity to ASTM standards. Analysis was performed via a Varian Inc. Vista-PRO Inductively Coupled Plasma Optical Spectrometer, with the exception of carbon and sulphur which were measured using a LECO Corp. Combustion Analysis system. Proprietary software and reference standards were used for data capture and analysis.

3.5.2 Nitrogen Analysis

Nitrogen is not part of the ASTM specification, it was analyzed, however since nitrogen is a well-known austenite stabilizer and it is commonly stated as the cause of retained austenite within existing literature. The nitrogen content was investigated to determine if variations existed between the TM and AM samples and to examine the influence of heat treatment on nitrogen levels. Analysis was performed via an Eltra ONH 2000 Inert Gas Fusion and Thermal Conductivity Detector using ASTM E1019-11 test method.

3.5.3 Particle Size, Distribution, and Shape

EOS does not provide specifications for particle size, distribution, or shape within their GP1 powder, however, based on the literature review in section 2.1.3 it is well-known that specific powder properties are required to achieve a high packing density and defect free parts.

Powder particle size and distribution analysis were performed using a Malvern Panalytical Mastersizer 2000 Laser Diffraction particle size analyzer. Proprietary software was used for data capture and analysis. Powder particle shape was first analyzed via a desktop inverted light microscope to produce optical magnification images. Subsequent Scanning Electron Microscope (SEM) images were taken via a JEOL Ltd. JSM-6610LV SEM utilizing an accelerating voltage of

10KeV, a working distance of 11mm, and a spot size of 53nm. Proprietary software was used for data capture and analysis.

3.5.4 Retained Austenite

Retained austenite has been repeatedly shown to be the cause of reduced mechanical properties within published literature. Fertiscope, X-Ray Diffraction (XRD), and Electron Backscatter Diffraction (EBSD) analysis methods were selected to evaluate retained austenite within the bulk, at and just beneath the surface, and at the immediate surface respectively. The purpose was to identify volume fractions of retained austenite after subsequent preparation and processing techniques and identify possible discrepancies between the various analytical techniques.

A Fertiscope was utilized for the evaluation of bulk retained austenite. Measurements were performed via a Metis Instruments & Equipment NV MSAT-30. The Helmholtz constant was calibrated to 0.0218cm and Magnetics Diagnostics was used for data capture and analysis

XRD was utilized for surface analysis of retained austenite with a limit penetration depth of approximately 30μm. Measurements were performed via Bruker D8 DISCOVER with DAVINCI.DESIGN diffractometer. A cobalt source was used and Bruker-AXS software suite was utilized for data capture and analysis. Rietveld analysis was performed using peaks (111), (002), (022), (311) and (222) for austenite identification and (110), (002), (211) and (220) for martensite identification.

EBSD was utilized for surface analysis of retained austenite with no penetration beyond the immediate surface layer. Measurements were performed on electropolished samples using a JEOL Ltd. JSM-7000F SEM. JEOL Ltd. utilizing an accelerating voltage of 10KeV, a working distance of 11mm, and a spot size of 53nm. Oxford Instruments HKL CHANNEL 5 software was used for

data capture and analysis. The EBSD analysis was performed using 4x4 binning and a 0.1-0.25 μm step size.

3.5.5 Grain Structure

Grain structure was evaluated to determine the influence of process parameters on the resulting microstructure. The same EBSD method outlined in section 3.5.4 for this analysis.

3.5.6 Dilatometry

Dilatometry was utilized to determine the transformation temperatures of the TM and AM alloys in their as-received and as-built conditions respectively. Measurements were performed via a BÄHR Thermoanalyse GmbH DIL 805 Quench-Deformation Dilatometer. The testing was performed by heating from ambient temperature to 1040°C under vacuum at a rate of 3.4°C/s, holding for 5 minutes, then cooling at a rate of 10°C/s using helium gas. The heating rate was performed according to test standards while cooling rate was selected to ensure sufficient cooling to allow martensitic transformation.

4. Experimental Results

Samples were analyzed to determine influences of process and preparation conditions on the composition, transition temperatures and phase present.

4.1. Chemical Analysis

Chemical characterization was performed according to section 3.5.1 with the results displayed in Table 7 along with the ASTM specification (ASTM International 2010). The results show all elements are within the ASTM specification, with the exception of chromium, which was slightly below the standard values. The chromium discrepancy will not influence the analysis as the reference and AM samples are within error of each other, hence lacking chromium will equally influence all samples. Interestingly, there was no significant difference between composition of the 17-4PH Powder and the AM samples in their as-built condition.

Sample	**Cr**	**Ni**	**Cu**	**Mn**	**Si**	**C**	**P**	**S**	**Nb+Ta**
ASTM Min	15.0	3.0	3.0	0.0	0.0	0.00	0.00	0.00	0.2
ASTM Max	17.0	5.0	5.0	1.0	1.0	0.07	0.04	0.03	0.5
Reference	14.1	4.2	3.2	0.8	0.4	0.03	0.02	0.03	0.3
17-4 Powder	14.4	4.3	4.3	0.8	0.5	0.06	0.01	0.01	0.2
AM-N2	14.6	4.6	4.3	0.7	0.5	0.07	0.01	0.01	0.3
AM-Ar	14.5	4.6	4.1	0.6	0.6	0.05	0.01	0.01	0.2

Table 7: ASTM composition specifications and measured compositions of wrought and printed specimens in wt%. The accuracy of the measured compositions is estimated at ± 2% of the measured concentration in the case of the substitutional elements. In the case of carbon and sulfur the values are within +/- 0.005 wt%.

4.2 Nitrogen Analysis

Nitrogen analysis was performed according to section 3.5.2 with the results displayed in Table 8. The results show there was no difference in the nitrogen content in AM samples that are processed under nitrogen or argon atmospheres. Solution annealing does not reduce the nitrogen content of any of the samples and the nitrogen content of AM samples is up to 0.12 wt% higher than that of the TM samples.

Sample	Ref.	Ref. +SA	17-4 Powder	AM-N2	AM-Ar	AM-N2+SA	AM-Ar+SA
N (wt%)	0.04	0.03	0.015	0.12	0.12	0.13	0.13

Table 8: Measured nitrogen content (wt%), of reference wrought 17-4PH material as well as AM powder and AM components manufactured and heat-treated under different conditions. The accuracy of the measurements is ±0.01wt%

4.3 Particle Size, Distribution, and Shape

Particle size and distribution was performed according to section 3.5.3 with the results displayed in Figure 7. The results show 50% of the particles have a diameter less 34µm, while 90% are less than 58µm according to ASTM B822 (ASTM International 2017).

Particle shape analysis was performed according to the procedure described in section 3.5.3 and with optical results being displayed in Figure 8. And SEM results displayed in Figure 9. The particles exhibited a consistent morphology with very few satellites.

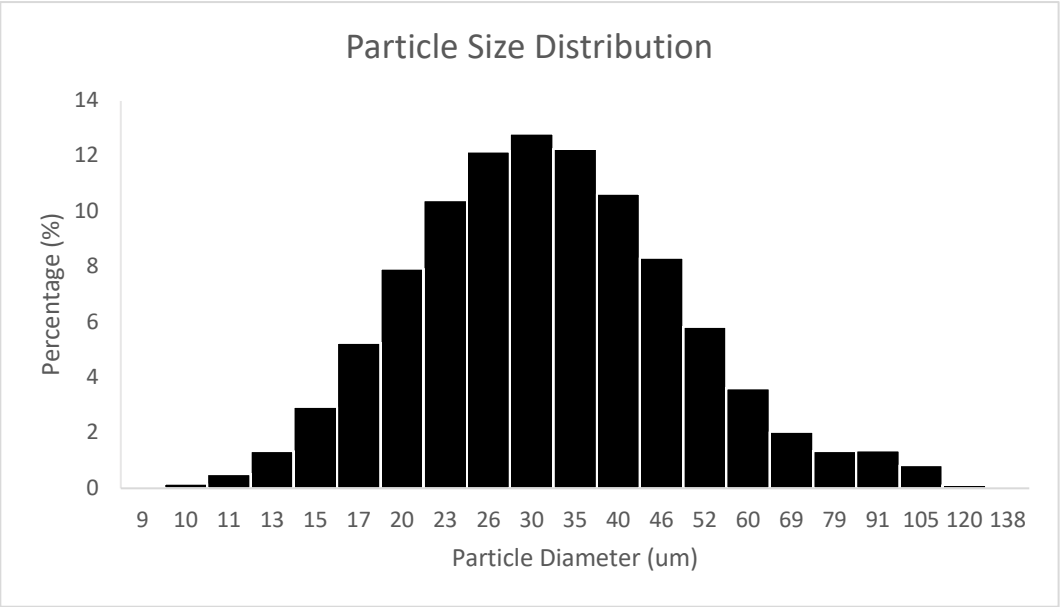

Figure 7: Particle size distribution 17-4PH powder, according to ASTM B822, reveals 50% of the particles have a diameter less 34μm, while 90% are less than 58μm

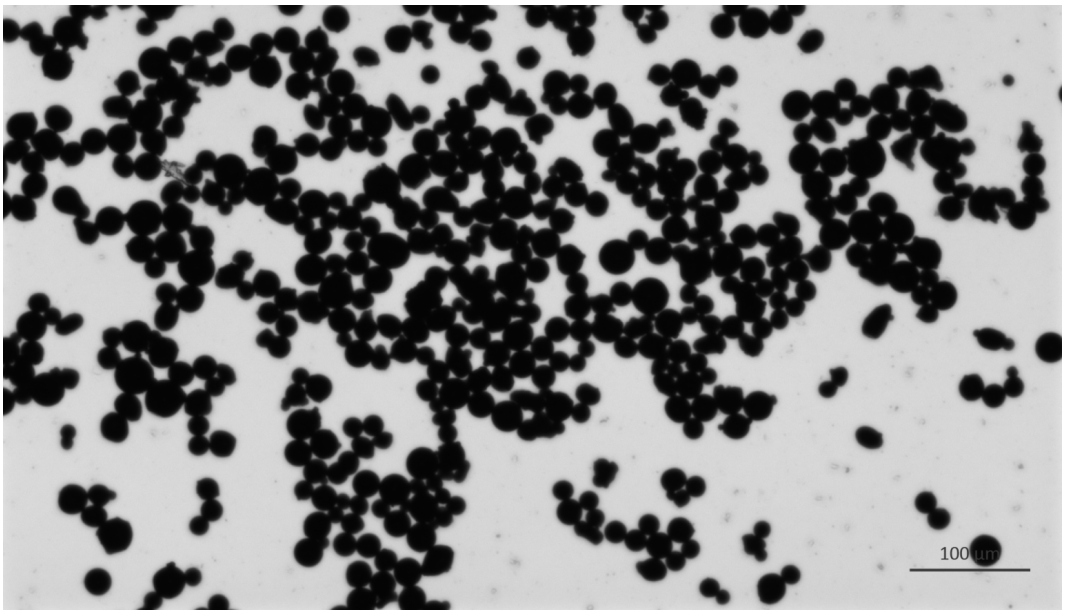

Figure 8: Optical images of 17-4PH powder demonstrating the consistency of particle size and shape

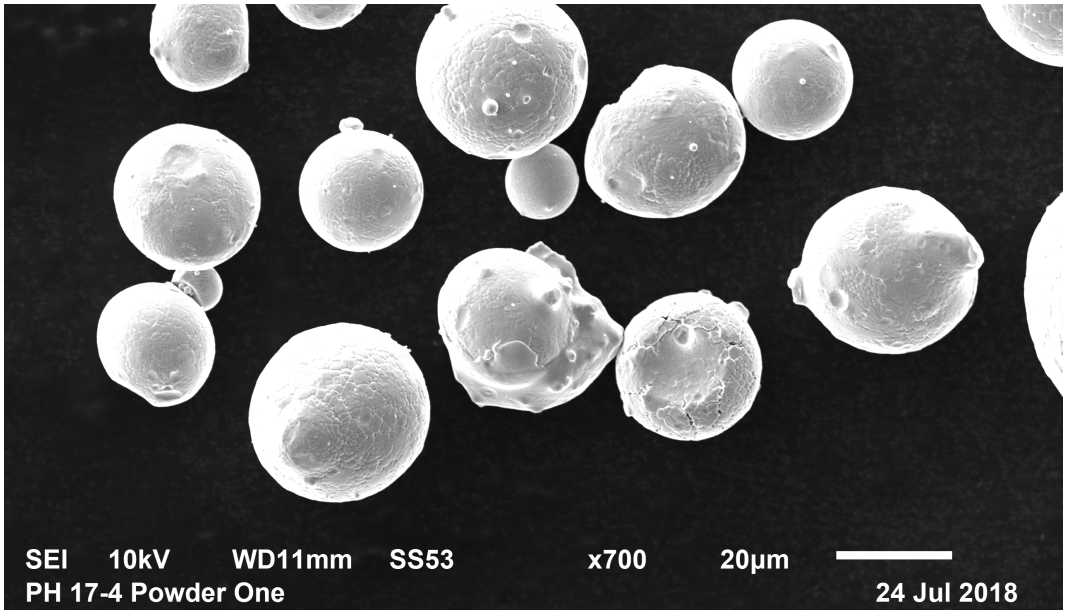

Figure 9: SEM images of 17-4PH powder demonstrating highly spherical particles with uniform surface morphology.

4.4 Retained Austenite

Retained austenite was analyzed via Fertiscope, for bulk measurements, and XRD and EBSD for surface measurements, with the results summarized in Table 9. Details of the experimental method are outlined in section 3.5.4.

The fertiscope results show there is no difference between the volume fractions of retained austenite for AM samples produced under nitrogen or argon process atmospheres. The amount of retained austenite was consistent between all samples, with the exception of those that underwent a deformation treatment. The amount of retained austenite was shown to decrease with increasing deformation. The XRD analysis is complicated by the presence of texture within some of the samples. Nonetheless, it is evident that there is no difference in the retained austenite fraction between the AM samples that are produced under nitrogen and those produced under argon process atmospheres, regardless of process and preparation conditions. Cryogenic treatment can reduce the

retained austenite to 82%. Polishing can reduce the retained austenite to 81%. Solution annealing and polishing can reduce the retained austenite to 53%. The EBSD results show there is no difference in the retained austenite in AM samples that are produced under nitrogen or argon process atmospheres while solution annealing shows the retained austenite can be reduced to 20%.

Sample	Fertiscope (%)	XRD (%)	EBSD (%)
Reference	7.9	4	n/a
17-4 Powder	99.7	98	n/a
AM-N2	99.7	98	n/a
AM-N2+SA	99.0	n/a	n/a
AM-N2-P	99.7	81	55
AM-N2+SA-P	99.0	53	15
AM-N2+SA+H900	98.9	n/a	n/a
AM-N2+LN2	99.6	90	n/a
AM-N2+R10	96.1	n/a	n/a
AM-N2+R30	64.3	n/a	n/a
AM-N2+R50	41.3	n/a	n/a
AM-Ar	99.3	96	n/a
AM-Ar+SA	99.0	n/a	n/a
AM-Ar-P	99.3	87	55
AM-Ar+SA-P	98.9	59	20
AM-Ar+SA+H900	99.0	n/a	n/a
AM-Ar+LN2	99.3	82	n/a
AM-Ar+R10	95.8	n/a	n/a

AM-Ar+R30	65.7	n/a	n/a
AM-Ar+R50	43.3	n/a	n/a

Table 9: Results of retained austenite volume fraction for fertiscope (±0.2%), XRD (±3%), and EBSD. Error of EBSD cannot be accurately measured but will be within ±3% based on image analysis.

4.5 Grain Structure

EBSD was performed utilizing the method outlined in section 3.5.5. The results of Figure 10a and 11a indicate there is no significant difference in the grain size, shape, or distribution in AM samples produced under nitrogen or argon process atmospheres. Figure 10b and 11b indicate that AM samples produced under nitrogen or argon process atmospheres will both exhibit a predominately martensitic microstructure after solution annealing on the surface.

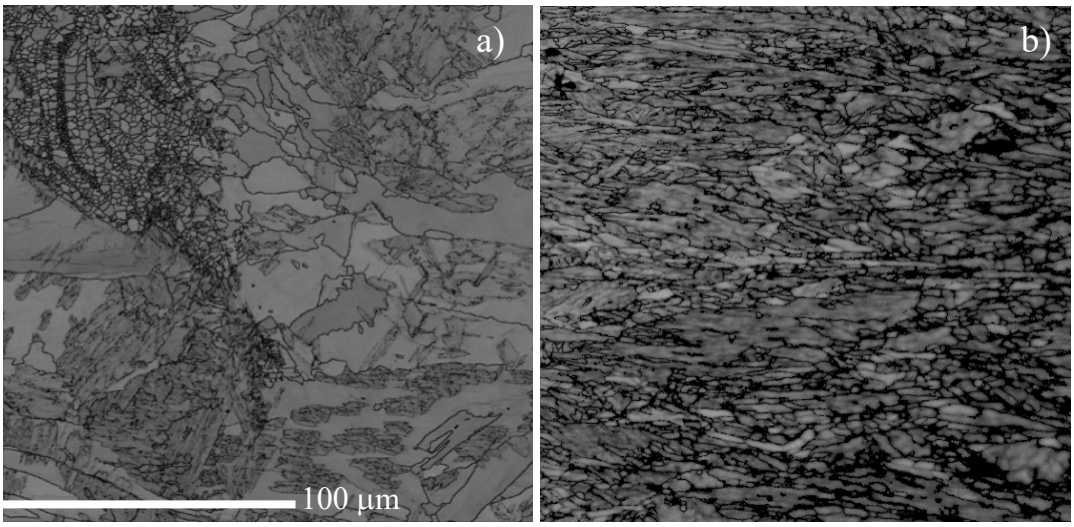

Figure 10: EBSD band contrast of AM samples produced under nitrogen after a) polishing showing a mix of large and fine grains b) solution annealing at 1040℃ and polishing showing fine grains associated with a martensitic structure

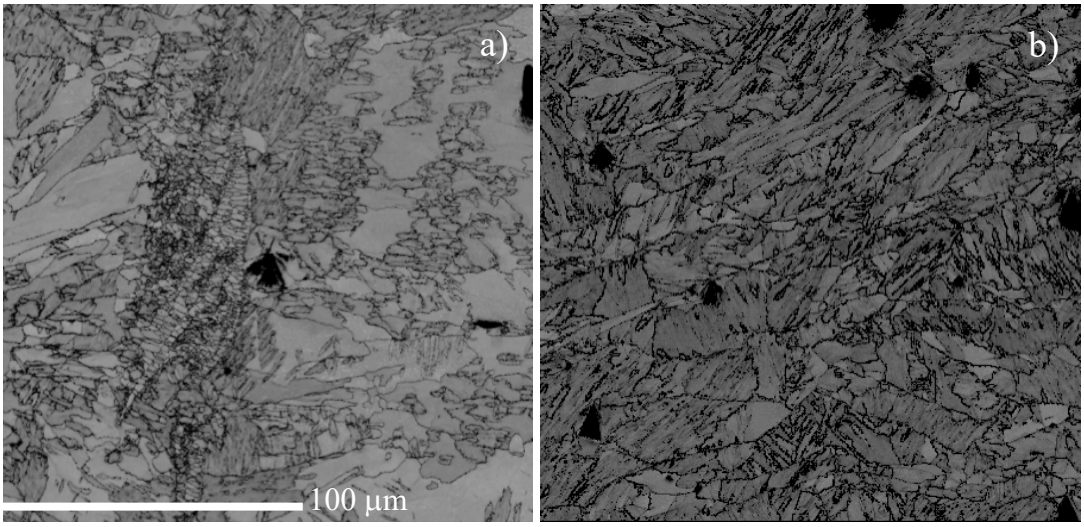

Figure 11: EBSD band contrast of AM samples produced under argon after a) polishing showing a mix of large and fine grains b) after solution annealing at 1040℃ and polishing showing fine grains associated with a martensitic structure

4.6 Dilatometry

Dialatometry analysis was performed according to section 3.5.6. The results in Figure 12 demonstrates that the TM sample exhibits a volume increase associated with a martensitic transformation upon cooling, with an approximate Ms=151°C. Figure 13 and Figure 14 demonstrates that the AM samples produced under nitrogen or argon process atmospheres do not exhibit a significant volume increase associated with a martensitic transformation upon cooling from solution annealing to ambient temperatures. The difference between initial and final length of the AM samples can be attributed to the austenitization of the martensite which was formed during sample machining.

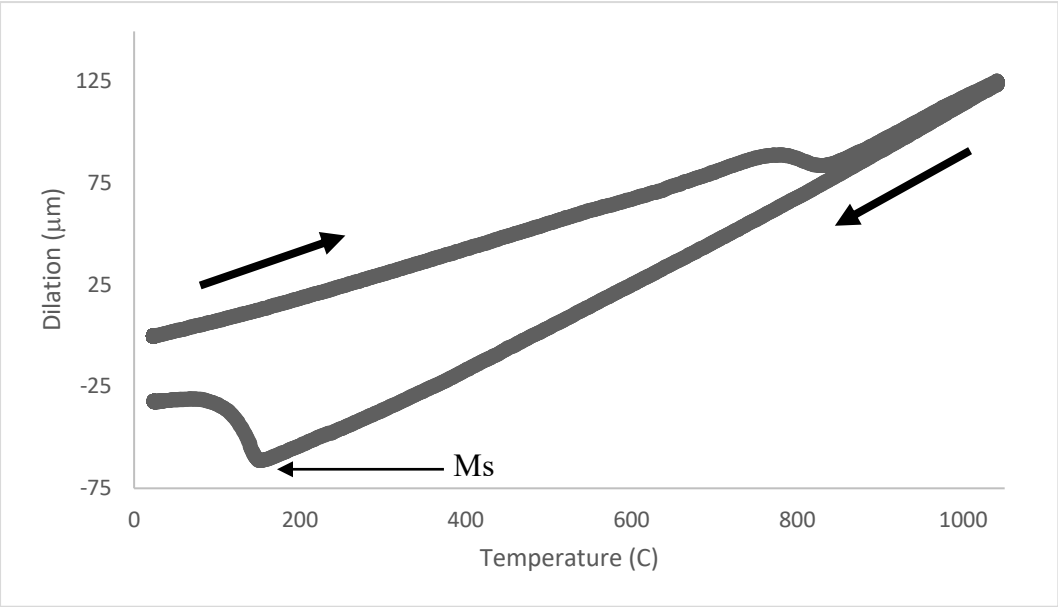

Figure 12: Dilatometry of reference sample exhibiting volume increase associated with a martensitic transformation upon cooling

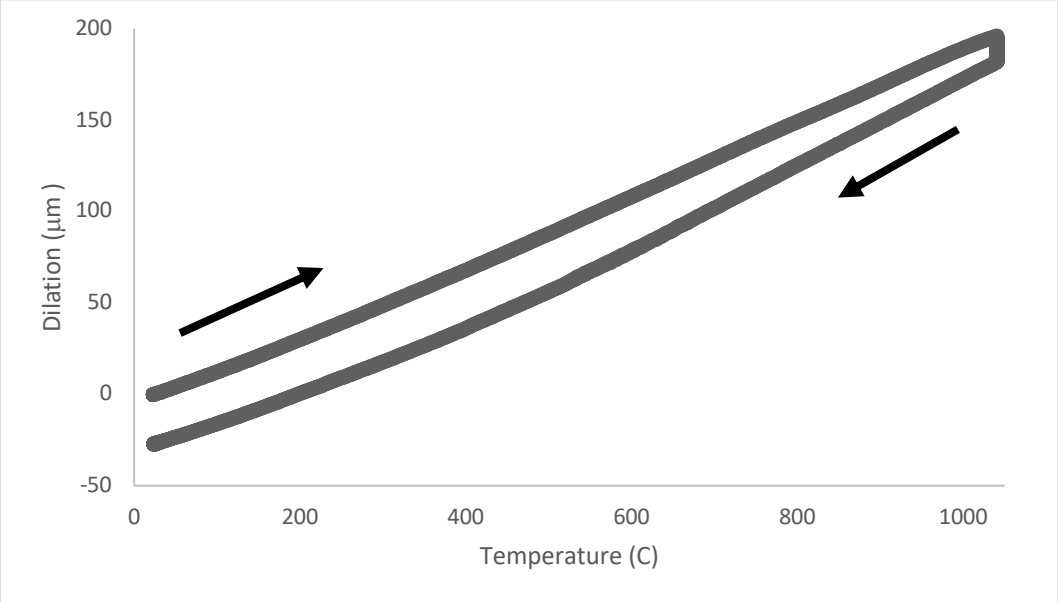

Figure 13: Dilatometry of AM sample produced in nitrogen atmosphere does not exhibit a volume increase associated with a martensitic transformation upon cooling

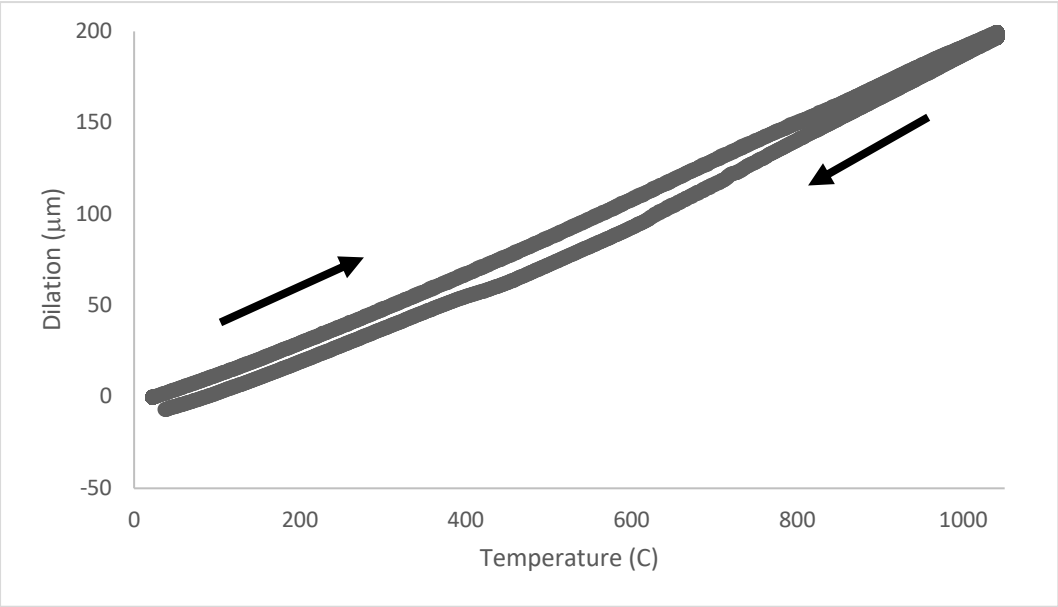

Figure 14: Dilatometry of AM sample produced in argon atmosphere does not exhibit a volume increase associated with a martensitic formation upon cooling

4.7 Summary

The composition of the materials utilized conforms to the ASTM specification, with the exception of chromium content which is slightly below the required values for all samples. The nitrogen content of the AM samples is at least 0.12wt% higher than that of the wrought alloy. This has the potential to reduce the Ms temperature and caused austenite to be retained at room temperature.

EOS does not provide specifications for particle size, distribution, or shape within their GP1 powder; however, the analysis performed shows the powder has been designed to remove both large and small particles. The remaining distribution allows for a high packing factor, permitting the creation of defect free parts. The highly spherical shape of the particles improves flowability of the powder within the process to ensure the high packing density can be achieved.

The analysis of retained austenite demonstrate very clear trends. Bulk analysis via fertiscope shows a predominately austenite phase. Changes to process atmosphere, sample preparation, and thermal treatment have no influence on the volume fraction of retained austenite. Deformation of the sample shows a reduction of the retained austenite indicating the presence of the TRIP phenomenon.

Surface analysis via XRD has a penetration depth of approximately 30μm, while EBSD evaluates the immediate surface. Both techniques show a decrease in retained austenite after the polishing process, however the EBSD shows 50% while XRD only shows 81%. Combining this with the fertiscope which shows no decrease in retained austenite after polishing confirms the presence of a surface transformation being imparted on the samples from the polishing process due to the TRIP phenomenon.

Solution annealing demonstrated even further decrease in retained austenite with EBSD showing 20%, XRD showing 53%, but fertiscope showing no charge. It is believed that the solution annealing allows for the formation of precipitates which reduces the nitrogen content in solution. The nitrogen is not reduced enough to destabilize the austenite at room temperature, however it is significant enough to make it less resistant to mechanical deformation allowing more transformation.

5 Discussion

Several items of note were found throughout the analysis of these AM samples. The influence of process atmosphere will be discussed in section 5.1, followed by further exploration into the influence of nitrogen on retained austenite in section 5.2. The TRIP phenomenon and its ability to influence surface analysis is discussed in 5.3, and finally an in-depth analysis of EOS datasheets is performed in section 5.4.

5.1 Influence of Process Atmosphere on Retained Austenite

The general consensus within the literature is that the AM processing atmosphere can directly control the resulting microstructure of a nitrogen atomized 17-4PH (Murr et al. 2012). Under a nitrogen processing atmosphere, it will produce an austenitic microstructure, while an argon atmosphere will produce a martensitic microstructure. This notion has become so prevalent that even AM powder manufacturers have published white papers reiterating this phenomenon (LPW Technology Ltd. 2017), unfortunately these results could not be reproduced and samples produced under either atmosphere resulted in similar microstructure and volume of retained austenite.

The SLM process has extremely high cooling rates (Vilaro, Colin, and Bartout 2011) which can result in formation of fine grains. These fine grains can inhibit the austenite to martensite transformation by reducing the Ms temperature (Yang and Bhadeshia 2009) which can result in retained austenite at ambient temperatures. The theory put forth is that argon has 40% lower thermal conductivity compared to nitrogen, producing slower cooling rates, allowing for the formation of larger grains and thereby less retained austenite at ambient (Murr et al. 2012). EBSD

micrographs in Figure 10 and Figure 11 show the resulting grain microstructure from nitrogen and argon processing atmospheres, respectively. Both clearly show the formation of fine grains, however there is not a significant difference in the grain size, shape, or distribution between the two. This leads us to discount the argument put forward by Mur et al. Furthermore, the difference between the thermal conductivity of Ar and N2 is 17.7 and 26.0 mW/m K respectively. This does not seem significant enough to modify the microstructure obtained during AM.

The XRD analysis in Table 9 shows that TM samples (Reference, Reference+CA) are predominately martensitic, which is the expected phase of this alloy. However, the AM samples in their as-built condition (17-4 Powder, AM-N2, and AM-Ar) are predominately austenitic. The fertiscope analysis in Table 9 supports these results.

The notion that by simply changing the AM processing atmosphere, one can control the resulting microstructure has been shown to be irreproducible and given the overall low thermal conductivity of both gases, illogical. The data collected demonstrates that a change in process atmosphere will not alter the amount of retained austenite.

5.2 Influence of Nitrogen on Retained Austenite

Several papers state that nitrogen is able to stabilize the austenitic phase at ambient temperatures. However they all subsequently assert that varying the AM process atmosphere (Rafi et al. 2014) or performing heat treatment (Starr et al. 2012), will result in a martensitic phase at room temperature. Given that it has now been shown that varying the AM process atmosphere will not alter the resulting microstructure, further investigation is needed into the influence of nitrogen on retained austenite and its stability within the alloy.

5.2.1 Origin of Nitrogen Content

As shown by the nitrogen analysis in Table 8, the 17-4PH powder and samples produced from it have up to 0.15 wt% nitrogen compared to less than 0.03 wt% in the TM samples. The gas atomization process utilizes high pressure nitrogen at elevated temperatures to produce highly spherical particles, the vast majority of which are 20-60um in size. Although this process is rapid, the high surface area of these particles and solubility of nitrogen within the liquid alloy allows abundant opportunity for nitrogen dissolution into the liquid, compared to a traditionally casting process.

5.2.2 Effect of Nitrogen on the Ms Temperature

It is well established that 17-4PH has a martensite finish just above ambient temperature (Davis 1994), therefore even small changes in composition could be enough to retain austenite at room temperature. Figure 12 shows the TM sample has a Ms temperature of approximately 151°C, which aligns with values published in the literature (Hsiao, Chiou, and Yang 2002). Figure 13 and Figure 14 show the AM samples, neither of which exhibited a martensitic transformation, indicating the Ms temperature is below room temperature.

There are numerous equations that evaluate the influence of composition on Ms temperature (Barbier 2014). Unfortunately no single existing equation can take all of the alloying elements of 17-4PH into consideration. However, the most commonly cited formula as shown in Equation 1 (Eichelmann G.H. 1953) can be used to approximate the change in Ms due to compositional differences between the reference sample and the 17-4PH powder.

$$Ms\ (℃) = 1302 - 42(wt\%Cr) - 61(wt\%Ni) - 33(wt\%Mn)$$

$$-28(wt\%Si) - 1667(wt\%[C + N]) \text{ ---(1)}$$

The result of this calculation shows 17-4PH powder has a decrease in Ms of over 250°C, of which, more than 180°C is attributed to the increase in nitrogen compared to the reference sample. This would push the Ms well below ambient temperatures resulting in an austenite being stabilized, confirming both the fertiscope and dilatometry analysis.

5.2.3 Nitrogen Stability within the Alloy

Due to the high Cr content of 17-4PH, nitrogen has a relatively high solubility within the austenite phase as shown in Figure 15, which was generated via Thermo-Calc Software (Thermo-Calc 2017a- TCFE6 database). It can be seen that up to 0.2wt% nitrogen is stable in solution at the solution annealing temperature of 1040°C. This is confirmed by the nitrogen analysis which shows solution annealing has little influence on the nitrogen content of the alloy.

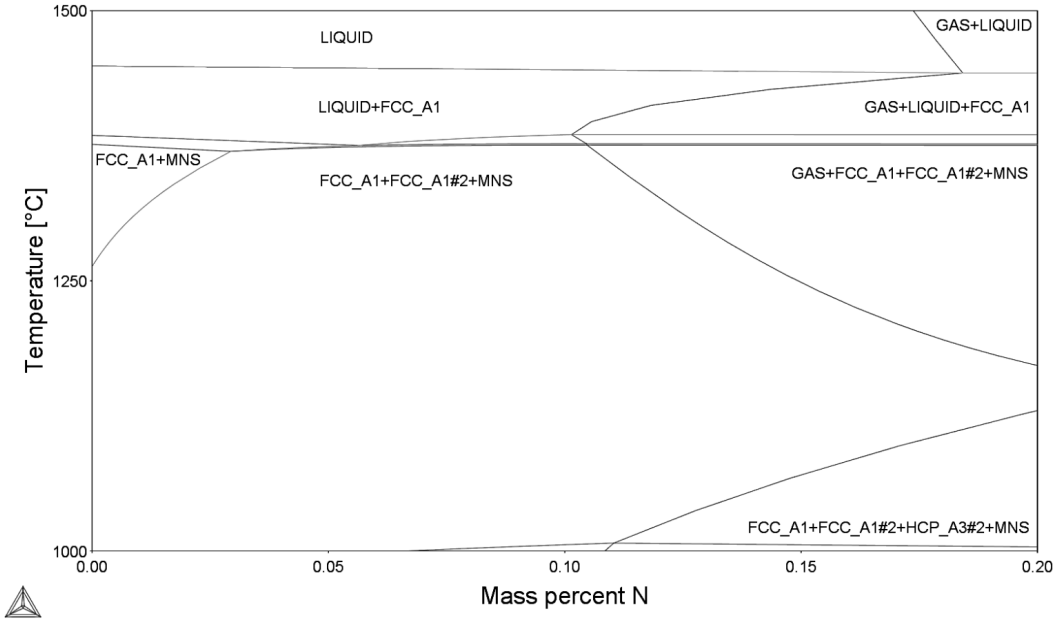

Figure 15: Phase Diagram of 17-4PH at 1atm pressure illustrating the stability of nitrogen in solution

5.2.4 Diffusion of Nitrogen

If nitrogen is stable within the alloy, the only way for it to be removed under heat treatment is through diffusion. If heat treatment is performed under vacuum or argon, as recommended by EOS, there will be a driving force for nitrogen to diffuse out of the material. The nitrogen concentration at the surface will depend on whether the denitriding process is controlled by bulk diffusion in austenite or by the recombination reaction at the surface. For the purpose of this discussion, the worst-case scenario is considered; the nitrogen concentration at the surface is assumed to be 0wt%. The diffusion profile in Figure 16 illustrates that after the 30 minute solution annealing cycle, the average nitrogen concertation of a 3 mm thick disk is 0.11wt%. Figure 17 shows that only the outer 0.1mm of material achieves a composition less than 0.04wt%. Thus, only a thin layer near the surface of the sample would be expected to transform to martensite as a result of denitriding during the solution treatment. The bulk of the sample will continue to have a high N content (low Ms) and should retain its austenitic microstructure at room temperature.

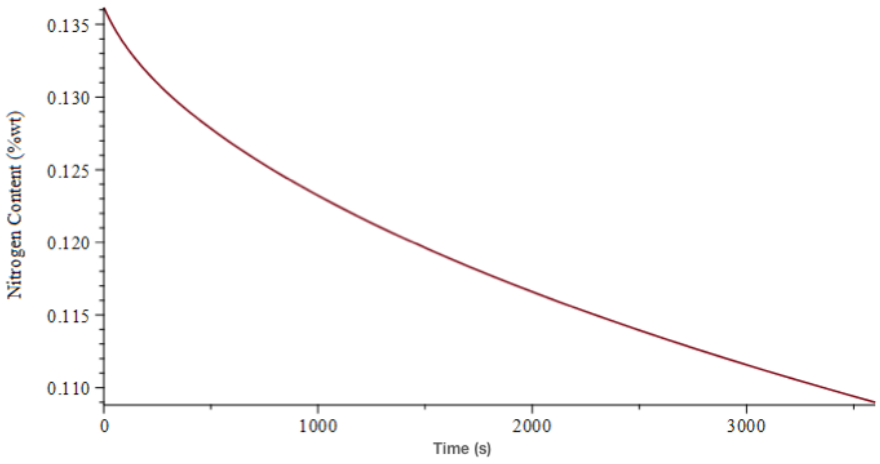

Figure 16: Average nitrogen content over time due of a 5mm thick cylinder with a nitrogen concentration of 0.14wt% within the bulk and 0.00wt% at the surface. A diffusion coefficient of 1.84x10-11m^2/s at 1040 ℃ was assumed for calculation.

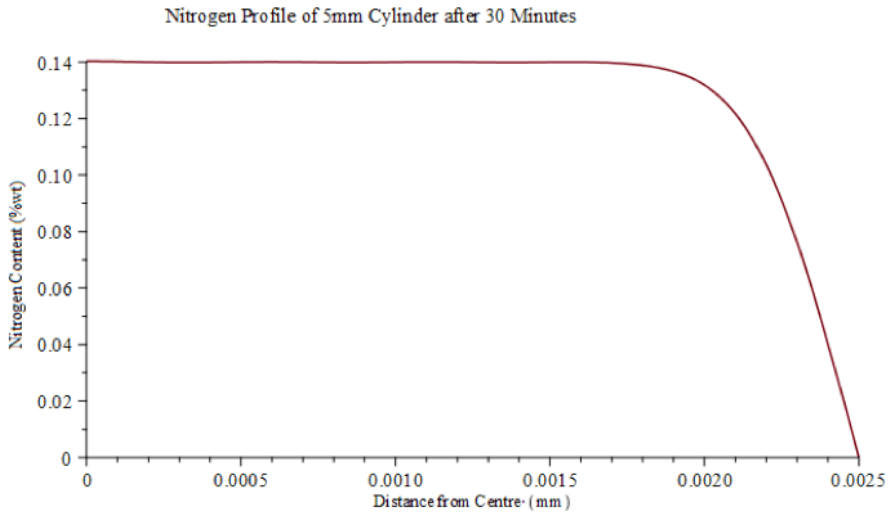

Figure 17: Nitrogen concentration profile of a 5mm sample after solution annealing at 1040℃ for 30minutes.

5.2.5 Summary

It is well established that nitrogen has the ability to stabilize austenite at low temperatures (Ul'yanin, Sorokina, and Zaretskii 1969). The utilization of a nitrogen gas atomization process and the higher surface area of the particles produced, allows abundant opportunity for nitrogen dissolution during gas atomization. An analysis of 17-4PH powder and AM samples confirms this, as they have up to 0.12wt% higher nitrogen content than the TM sample.

The additional nitrogen alone contributes to a Ms temperature decrease of more than 180°C. Given the reference sample has a Ms of 151°C, this pushes the Ms of the AM samples well below ambient temperatures making it possible to retain austenite at room temperature, which is supported by fertiscope and dilatometry analysis. Performing heat treatment under vacuum or argon can theoretically allow denitriding to occur, resulting in up to 0.1mm of the outer surface exhibiting a martensitic transformation. However, this is an extreme case under ideal conditions; in practical application the results would have a significantly lower depth of penetration.

5.3 Influence of Deformation on Retained Austenite

It is widely accepted that the retained austenite within SLM 17-4PH is metastable, and that it transforms to martensite when deformed (Facchini et al. 2010). The data collected supports these claims by demonstrating application of bulk deformation will reduce the volume of retained austenite in Section 5.3.1. Additionally, numerous situations are outline in Section 5.3.2 in which unintentional deformation can occur, such as mounting and polishing, which result in a significant decrease in retained austenite at the surface when measured by XRD.

5.3.1 Applied Deformation

The deformation treatment reduced the thickness of the samples by 10%, 30%, and 50% resulting in the retained austenite decreasing by 4%, 35%, and 58% respectively, as shown by fertiscope results in Table 9. This demonstrates that with increasing deformation the retained austenite will progressively transform to martensite.

5.3.2 Unintentional Deformation

After the SLM process is complete, a sample is separated from a build platform through manual or automated machining processes. Additional machining is also required for the removal of excess support structure. These machining processes have the potential to introduce stress and deformation to the outer surface as it removes material.

It is also common practice after samples are produced, to use a sandblasting process to smooth the surface of the parts and to remove any excess powder that remained after the SLM process. This sandblasting process would introduce a compressive stress to the outer surface of the material.

The fertiscope results in Table 9 show a negligible change in the AM samples' retained austenite content compared to their as-built counterparts, regardless of preparation process. This is supported by the dilatometry results in Figure 13 and Figure 14, which showed that the AM samples will not form martensite during cooling. It is interesting to point out that the dilatometer samples post processing to remove them from the build platform, and should therefore contain martensite. The heating and holding portions of the dilatation curve, however, suggest that the martensite formed during machining transforms to austenite during heating as suggested by the decrease in specimen length. Therefore, the dilatometer experiments provide reliable results in spite of the fact that some martensite was initial present due to post processing.

Variation in the amount of retained austenite was observed in XRD results while evaluating the samples after each preparation process. Table 9 shows that by mounting and polishing the AM samples, the retained austenite can be reduced to 81% from its as-built condition. Furthermore, solution annealing the retained austenite can be reduced to 53% from its as-built condition. EBSD results in Table 9 also showed retained austenite can be reduced to 20% by solution annealing. The grinding and polishing will result in local deformation at the surface of the samples. This has potential to result in a transformation of the outer surface of the material.

5.3.3 Summary

The TRIP phenomenon is not present within traditional 17-4PH. However, the data collected aligns with published literature in that retained austenite within AM 17-4PH will transform to martensite due to the TRIP phenomenon. Subjecting AM samples to cold rolling shows that with increasing deformation the amount of retained austenite is reduced.

Dilatometry establishes that the AM samples do not exhibit a martensitic transformation on cooling. This is further reiterated by the fertiscope results that demonstrate a negligible change in retained austenite regardless of sample production and preparation process. However, XRD and EBSD show reductions in retained austenite of up to 85% as a result of the AM sample preparation process. Literature reveals that grinding and polishing can cause deformation resulting in residual stress to depths of 0.2mm within austenitic stainless steels (Ding et al. 2017). This would result in a surface transformation quantifiable by sensitive surface analytical techniques like XRD and EBSD but not significant enough to be detected by bulk analytical techniques like dilatometry and fertiscope.

Given that the majority of literature performed their phase identification via XRD, the variation in retained austenite measurements can be attributed to the extent of the surface transformation the authors imparted on their AM samples during the preparation process.

5.4 Manufacturers Datasheets

Since 2007, EOS has released 3 different versions of 17-4PH stainless steel; “EOS StainlessSteel GP1”, “EOS StainlessSteel 17-4PH”, and “EOS StainlessSteel 17-4PH IndustryLine” all of which have the same chemical composition and powder size, based on the supplied material datasheets. With each subsequent release, EOS updates their post processing procedures.

5.4.1 EOS StainlessSteel GP1

EOS StainlessSteel GP1 (EOS GmbH - Electro Optical Systems 2009) provides very little details regarding post processing of the printed parts. Stress relieving is recommended for 1 hour at 650 °C, however it makes a negligible difference in the tensile strength, yield strength, or elongation.

The hardness values provide interesting insight; a value of 230HV is reported for the as-built state, compared to 250-400 HV for the "ground & polished" state. This aligns with the data presented that the surface of the material will transform from austenite to martensite during grinding and polishing due to the TRIP phenomenon. EOS had misidentified this as a work hardening.

5.4.2 EOS StainlessSteel 17-4PH

EOS StainlessSteel 17-4PH (EOS GmbH - Electro Optical Systems 2015) states similar as-built mechanical properties. It does, however, recommend solution annealing followed by H900 precipitation hardening to achieve mechanical properties within the ASTM specifications for traditional 17-4PH. However, the data collected from the fertiscope results in Table 9 show that the material is predominately austenitic after this heat treatment procedure. Additionally this directly contradicts the earlier publications by EOS that stated: "austenite conditioning (solution treatment) followed by transformation cooling (quenching or air cooling) and then precipitation hardening, e.g. at 482°C (900°F) actually reduced the tensile strength instead of increasing it" (Shellabear and Nyrhilä 2007).

5.4.3 EOS StainlessSteel 17-4PH IndustryLine

EOS StainlessSteel 17-4PH IndustryLine (EOS GmbH - Electro Optical Systems 2017) also states similar as-built mechanical properties but provides two different heat treatment methods to achieve mechanical properties within the ASTM specifications. The first is solution annealing followed by H900 precipitation hardening, both performed under vacuum. The second is solution annealing followed by a modified precipitation hardening of 460°C for 1 hour, both performed under argon. These procedures are more or less identical to EOS StainlessSteel 17-4PH, and produce only marginally higher mechanical properties. However, EOS now explicitly states that heat treatment

should be performed under vacuum and if performed in atmospheric conditions, argon is preferred. It has been shown in section 5.2.3 the change in atmosphere would cause very little diffusion to occur, if any, making this change ineffective in altering the bulk of the sample.

5.4.4 Summary

The material datasheets from EOS provide an interesting if not confusing story. Originally EOS stated it was not possible for DMLS 17-4PH stainless steel to achieve mechanical properties within the ASTM specification through the use of solution annealing and precipitation hardening. The data collected reflects this, as the material is predominately austenitic according to fertiscope measurements in Table 9 when subjected to solution annealing or precipitation hardening.

EOS later stated that solution annealing and precipitation hardening can achieve mechanical properties within the ASTM specification, with the use of vacuum or argon further improving mechanical properties. However, it has been demonstrated that this change will allow for very limited diffusion to occur on the surface resulting in a negligible change to the bulk of the sample when compared to heat treatment in air.

One explanation for the claims made by EOS regarding the effectiveness of heat treatment would be the mechanism of precipitation. The phase diagram presented in Figure 15 demonstrates at 1040°C precipitation of niobium carbonitrides is possible, however the rapid cooling rates of the SLM process does not provide an opportunity for equilibrium to be reached leaving these elements in solution. Subsequent heat treatment could provide an opportunity for the above nitrides to form, thereby reducing overall nitrogen content in solution within the austenite phase and allowing martensite formation during cooling. Thermodynamic calculations demonstrate that at equilibrium the nitrogen and carbon content will be reduced to 0.064 wt% and 0.0037 wt%, respectively. This

significant reduction in austenite stabilizing elements would drastically increase the Ms temperature pushing it above ambient. The ASTM specifications, and EOS recommendations, do not provide details regarding the heating and cooling rates, providing an opportunity for variance to occur. The sample could be placed within the furnace, after which the furnace could be turned on and heated from room temperature to 1040°C. This would provide significantly more time at elevated temperature compared to placing the sample within a furnace that was already pre-heated to 1040°C. This is believed to be the origin of the inconsistencies reported with respect to the effect of solution treatment on the amount of martensite in the microstructure.

6 Conclusion

Contrary to earlier reports, the microstructure of AM samples produced from nitrogen atomized 17-4PH alloy cannot be manipulated by altering the SLM process atmosphere. This is demonstrated by the use of a fertiscope, which reveals a predominately austenitic microstructure within the AM samples produced in both nitrogen and argon process atmospheres. Dilatometry reiterates this by revealing the austenitic microstructure is retained at ambient temperatures and does not exhibit a martensitic transformation.

The austenitic microstructure was stabilized through the introduction of nitrogen during the gas atomization process, which has up to 0.12wt% higher nitrogen content than the TM samples. If solution annealing is performed under vacuum or within an argon atmosphere, it could cause nitrogen loss at the surface. However, the impact of denitriding was shown to be small and unlikely to have a significant influence in a practical application.

When subjected to deformation the retained austenite within the AM samples will transform to martensite. With bulk deformation techniques the retained austenite can be reduced by more than 50%. However, unintentional deformation as a result of sample production and preparation will result in a surface transformation that is easily detectable through surface analysis.

Variation within published literature is a product of the sample production and preparation due to the TRIP phenomenon. The numerous steps and parameters utilized all have the potential to cause a surface transformation which is easily detectable by XRD, the primary analytical method utilized by most authors for phase identification.

It is proposed that the rapid cooling rates of the SLM process result in the equilibrium state not be achieved and all nitrogen retaining in solution, pushing Ms below room temperature. Subsequent heat treatment provides an opportunity for the formation of nitrides, thereby removing nitrogen from solution and pushing the Ms above room temperature. However, the correct heating rates are not defined or well understood, and the reduction of austenite could not be achieved through heat treatment employed in the present study.

6.2 Future Work

Future work will focus on testing the hypothesis that nitride precipitation during solution treatment at 1040oC, reduces austenite stability and allows martensite formation during cooling. The focus will be on identifying the effecting of heating-rate and holding time on the precipitation kinetics and the time evolution of N content in austenite.

Other experiments are planned to compare the behavior of the TM and AM materials. A TM sample can be subjected to a nitriding process to bring its nitrogen content up to 0.14wt%. At this point the sample should exhibit the same level of retained austenite that has been shown within existing AM samples. Since the nitrogen is introduced during the gas atomization process, by switching the atomizing gas to argon it would prevent the absorption of additional nitrogen within the alloy. When the resulting powder is used to produce AM samples, they would exhibit a traditional martensitic microstructure. Starr et al. performed analysis on argon atomized powder confirming the printed parts result in a martensitic structure, however given the variability within literature its validity is questionable (Starr et al. 2012).

Evaluation of Ms temperature against nitrogen content could be performed. This would determine the level of nitrogen that is tolerable within the alloy before it reduces the Ms temperature below ambient. Manufacturers would then be able to control the gas mixture used within the atomization process to ensure these levels are not exceeded to ensure traditional mechanical behavior from this alloy.

Since this material can exhibit a surface transformation through the use of two different methods, it allows for the creation of functionally graded materials. Leveraging the TRIP phenomenon through the use of surface deformation methods such as shot peening, will generate a hardened outer surface. Through means of a nitriding process, the outer surface can also be hardened but in a more controlled manner.

There are several areas of further work that would be warranted. Verification of the TRIP and diffusion through additional test methods. Denitriding of a AM material to determine if it will exhibit similar behavior. And finally looking into ways to exploit the unique behavior of the alloy through the creation of functionally graded materials.

References

Additively AG. 2018. “Laser Melting.” Accessed July 19. https://www.additively.com/en/learn-about/laser-melting.

AK Steel Corporation. 2007. “17-4 PH.” https://www.aksteel.com/sites/default/files/2018-01/174ph201706.pdf.

AlMangour, Bandar, and Jenn-Ming Yang. 2017. “Understanding the Deformation Behavior of 17-4 Precipitate Hardenable Stainless Steel Produced by Direct Metal Laser Sintering Using Micropillar Compression and TEM.” *The International Journal of Advanced Manufacturing Technology* 90 (1–4). The International Journal of Advanced Manufacturing Technology: 119–26. doi:10.1007/s00170-016-9367-9.

ASTM International. 2010. “Standard Specification for Hot-Rolled and Cold-Finished Age-Hardening Stainless Steel Bars and Shapes.” doi:10.1520/A0276-10.2.

———. 2012. “Standard Terminology for Additive Manufacturing Technologies.” doi:10.1520/F2792-12A.

———. 2015. “Standard Test Methods and Definitions for Mechanical Testing of Steel Products.” doi:10.1520/A0370-14.2.

———. 2017. “Standard Test Method for Particle Size Distribution of Metal Powders and Related Compounds by Light Scattering.” doi:10.1520/B0822-17.

Averyanova, M., Ph. Bertrand, and B. Verquin. 2011. “Studying the Influence of Initial Powder Characteristics on the Properties of Final Parts Manufactured by the Selective Laser Melting Technology.” *Virtual and Physical Prototyping* 6 (April 2016): 215–23.

doi:10.1080/17452759.2011.594645.

Barbier, David. 2014. “Extension of the Martensite Transformation Temperature Relation to Larger Alloying Elements and Contents.” *Advanced Engineering Materials* 16 (1): 122–27. doi:10.1002/adem.201300116.

Cheruvathur, Sudha, Eric A. Lass, and Carelyn E. Campbell. 2016. “Additive Manufacturing of 17-4 PH Stainless Steel: Post-Processing Heat Treatment to Achieve Uniform Reproducible Microstructure.” *JOM* 68 (3): 930–42. doi:10.1007/s11837-015-1754-4.

Cooke, April, and John Slotwinski. 2015. “Properties of Metal Powders for Additive Manufacturing: A Review of the State of the Art of Metal Powder Property Testing.” *Additive Manufacturing Materials: Standards, Testing and Applicability*, 21–48. doi:10.6028/NIST.IR.7873.

Davis, J.R. 1994. *ASM Specialty Handbook: Stainless Steels*.

Dawes, By Jason, and Robert Bowerman. 2015. “Introduction to the Additive Manufacturing Powder Metallurgy Supply Chain.” *Johnson Matthey Technology Review* 59 (3): 243–56. doi:http://dx.doi.org/10.1595/205651315X688686.

Ding, Wenfeng, Liangchi Zhang, Zheng Li, Yejun Zhu, Honghua Su, and Jiuhua Xu. 2017. “Review on Grinding-Induced Residual Stresses in Metallic Materials.” *International Journal of Advanced Manufacturing Technology* 88 (9–12). The International Journal of Advanced Manufacturing Technology: 2939–68. doi:10.1007/s00170-016-8998-1.

Eichelmann G.H., Hull F.C. 1953. “The Effect of Composition on the Temperature of Spontaneous Transformation of Austenite to Martensite in 18-8 Type Stainless Steel.” *Transactions ASM* 45: 77–104.

EOS GmbH - Electro Optical Systems. 2009. “EOS StainlessSteel GP1.” https://www.eos.info/en.

———. 2015. “EOS StainlessSteel 17-4PH.” https://www.eos.info/en.

———. 2017. “EOS StainlessSteel 17-4PH IndustryLine.” https://www.eos.info/en.

Facchini, Luca, Nério Vicente, Ivan Lonardelli, Emanuele Magalini, Pierfrancesco Robotti, and Molinari Alberto. 2010. “Metastable Austenite in 17-4 Precipitation-Hardening Stainless Steel Produced by Selective Laser Melting.” *Advanced Engineering Materials* 12 (3): 184–88. doi:10.1002/adem.200900259.

Fritsching, Udo, and Volker Uhlenwinkel. 2012. “Hybrid Gas Atomization for Powder Production.” In *Powder Metallurgy*, edited by Ksenija Pesek, 99–124. InTech. doi:10.5772/35807.

Gu, Hengfeng, Haijun Gong, Deepankar Pal, Khalid Rafi, Thomas Starr, and Brent Stucker. 2013. “Influences of Energy Density on Porosity and Microstructure of Selective Laser Melted 17-4PH Stainless Steel.” In *Proceedings of Solid Freeform Fabrication Symposium*. Austin.

Hsiao, C. N., C. S. Chiou, and J. R. Yang. 2002. “Aging Reactions in a 17-4 PH Stainless Steel.” *Materials Chemistry and Physics*. doi:10.1016/S0254-0584(01)00460-6.

Jacob, Gregor, Christopher U Brown, M Alkan Donmez, Stephanie S Watson, and John Slotwinski. 2017. “Effects of Powder Recycling on Stainless Steel Powder and Built Material Properties in Metal Powder Bed Fusion Processes.” Gaithersburg, MD. doi:10.6028/NIST.AMS.100-6.

LeBrun, Tyler, Takayuki Nakamoto, Keitaro Horikawa, and Hidetoshi Kobayashi. 2015. “Effect of Retained Austenite on Subsequent Thermal Processing and Resultant Mechanical Properties of Selective Laser Melted 17-4 PH Stainless Steel.” *Materials and Design* 81.

Elsevier Ltd: 44–53. doi:10.1016/j.matdes.2015.05.026.

LPW Technology Ltd. 2018. “Powder Production.” Accessed April 18. https://www.lpwtechnology.com/technical-library/powder-production/.

———. 2017. “Nitrogen vs Argon Atomisa on of 17-4 PH Stainless Steel and Its e Ects on AM Processing.” https://www.lpwtechnology.com/wp-content/uploads/2017/04/Case-Study-10-Ar-vs-N-atomisation-1.pdf.

Mahmoudi, Mohamad, Alaa Elwany, Aref Yadollahi, Scott M. Thompson, Linkan Bian, and Nima Shamsaei. 2017. “Mechanical Properties and Microstructural Characterization of Selective Laser Melted 17-4 PH Stainless Steel.” *Rapid Prototyping Journal* 23 (2): 280–94. doi:10.1108/RPJ-12-2015-0192.

Murr, Lawrence E., Edwin Martinez, Jennifer Hernandez, Shane Collins, Krista N. Amato, Sara M. Gaytan, and Patrick W. Shindo. 2012. “Microstructures and Properties of 17-4 PH Stainless Steel Fabricated by Selective Laser Melting.” *Journal of Materials Research and Technology* 1 (3). Elsevier: 167–77. doi:10.1016/S2238-7854(12)70029-7.

Rafi, H. Khalid, Deepankar Pal, Nachiket Patil, Thomas L. Starr, and Brent E. Stucker. 2014. “Microstructure and Mechanical Behavior of 17-4 Precipitation Hardenable Steel Processed by Selective Laser Melting.” *Journal of Materials Engineering and Performance* 23 (12): 4421–28. doi:10.1007/s11665-014-1226-y.

Rashid, R., S.H. Masood, D. Ruan, S. Palanisamy, R.A. Rahman Rashid, and M. Brandt. 2017. “Effect of Scan Strategy on Density and Metallurgical Properties of 17-4PH Parts Printed by Selective Laser Melting (SLM).” *Journal of Materials Processing Technology* 249 (May). Elsevier: 502–11. doi:10.1016/j.jmatprotec.2017.06.023.

Shellabear, M, and O Nyrhilä. 2004. “DMLS – Development History and State of the Art.” In *Proceedings of the 4th International Conference on Laser Assisted Net Shape Engineering, Lane 2004*. Erlangen.

———. 2007. “Advances in Materials and Properties of Direct Metal Laser-Sintered Parts.” In *Proceedings of the 5th International Conference on Laser Assisted Net Shape Engineering, LANE 2007*. Erlangen. http://www.rm-platform.com/index.php.

Simchi, a. 2004. “The Role of Particle Size on the Laser Sintering of Iron Powder.” *Metallurgical and Materials Transactions B* 35 (5): 937–48. doi:10.1007/s11663-004-0088-3.

Starr, Thomas, Khalid Rafi, Brent Stucker, and Christopher Scherzer. 2012. “Controlling Phase Composition in Selective Laser Melted Stainless Steels.” In *Proceedings of the Solid Freeform Fabrication Symposium*, 439–46.

Sutton, Austin T., Caitlin S. Kriewall, Ming C. Leu, and Joseph W. Newkirk. 2017. “Powder Characterisation Techniques and Effects of Powder Characteristics on Part Properties in Powder-Bed Fusion Processes.” *Virtual and Physical Prototyping* 12 (1): 3–29. doi:10.1080/17452759.2016.1250605.

Ul’yanin, E. A., N. A. Sorokina, and Ya. M. Zaretskii. 1969. “Properties of Austenitic Steel with Nickel and Nitrogen at Low Temperatures.” *Metal Science and Heat Treatment* 11 (9): 681–82. doi:10.1007/BF00653157.

Vilaro, T., C. Colin, and J. D. Bartout. 2011. “As-Fabricated and Heat-Treated Microstructures of the Ti-6Al-4V Alloy Processed by Selective Laser Melting.” *Metallurgical and Materials Transactions A: Physical Metallurgy and Materials Science*. doi:10.1007/s11661-011-0731-y.

Wohlers, Terry, and Tim Gornet. 2014. "History of Additive Manufacturing." *Wohlers Report 2014 - 3D Printing and Additive Manufacturing State of the Industry*.

Yadollahi, Aref, Nima Shamsaei, Scott M. Thompson, Alaa Elwany, and Linkan Bian. 2017. "Effects of Building Orientation and Heat Treatment on Fatigue Behavior of Selective Laser Melted 17-4 PH Stainless Steel." *International Journal of Fatigue* 94 (January): 218–35. doi:10.1016/j.ijfatigue.2016.03.014.

Yang, Hong Seok, and H. K D H Bhadeshia. 2009. "Austenite Grain Size and the Martensite-Start Temperature." *Scripta Materialia* 60 (7). Acta Materialia Inc.: 493–95. doi:10.1016/j.scriptamat.2008.11.043.

Yap, C. Y., C. K. Chua, Z. L. Dong, Z. H. Liu, D. Q. Zhang, L. E. Loh, and S. L. Sing. 2015. "Review of Selective Laser Melting: Materials and Applications." *Applied Physics Reviews* 2 (4). doi:10.1063/1.4935926.

Appendix A

Additive Manufacturing Parameters

The parameters utilized in the AM process are outlined in Table 10, Figure 18, and Figure 19. The AlSi10Mg parameter set was utilized to allow access to the external gas input, as the manufacturers' GP1 parameters can only operate with the internal nitrogen generator.

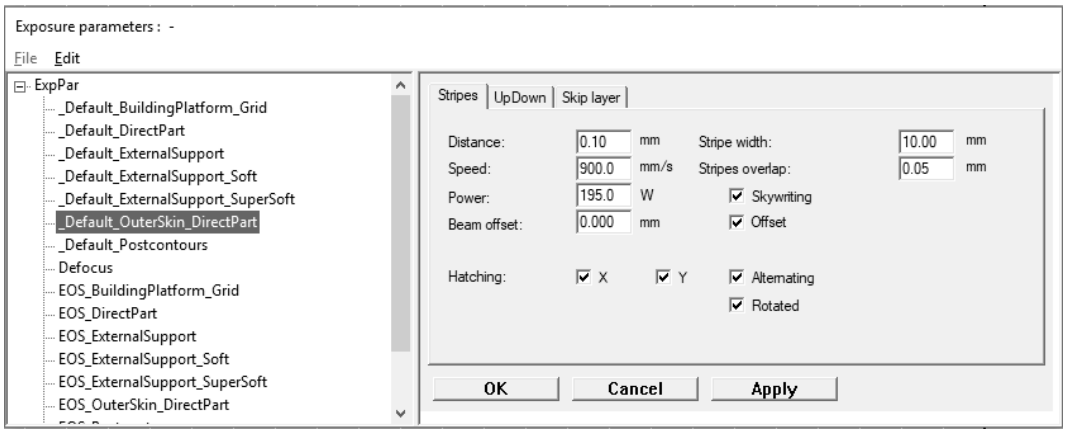

Figure 18: Additive manufacturing software parameters - strips

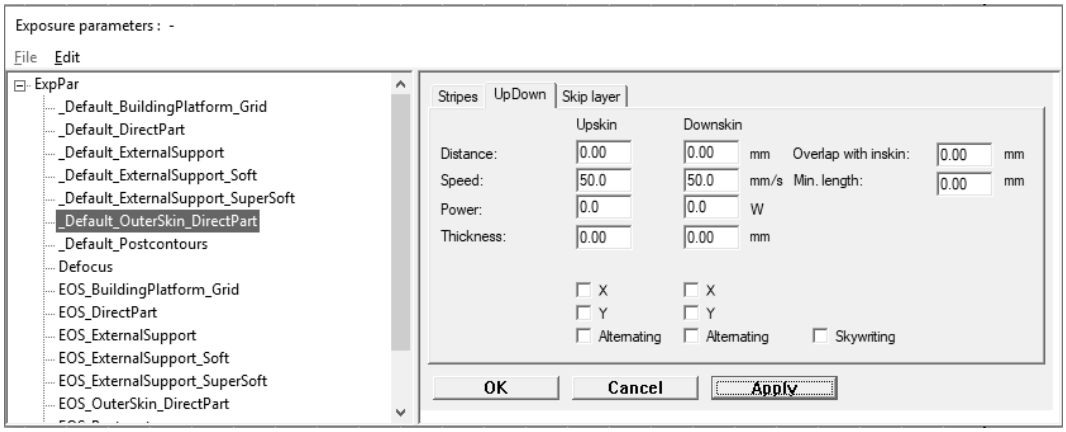

Figure 19: Additive manufacturing software parameters - up/down skin

Batch	1	2
Atmosphere	nitrogen	Argon
Beam Expander	0	
Beam Diameter (um)	100	
Gas Flow Rate (l/hr)	1000	
FRS Voltage (V)	2.5	
Material	EOS Stainless Steel GP1	
Material Lot #	F0301501-1	
Parameter Set	AlSi10Mg_030_110 Speed	
Layer Thickness (um)	40	
Build Platform Temp. ºC	35	
Exposure Type	_Default_OuterSkin_DirectPart	
Power (W)	195	
Speed (mm/s)	900	
Skywritting	Yes	
Offset	Yes	
Hatching (mm)	0.1	
Hatching Pattern	X, Y, Alternating, Rotated	
Strip Width (mm)	10	
Stripe Overlap (mm)	0.05	

Table 10: Additive manufacturing parameters used in this study.

Appendix B

Polishing Parameters

The parameters utilized for polishing is outlined in Table 11.

Step	**1**	**2**	**3**	**4**	**5**	**6**	**7**
Surface	SiC #500	SiC #800	SiC #1200	DAC*	Mol*	Nap*	Nap*
Suspension				DP-A 9um~	DP-A 3um~	DP-A 1um~	0.5um`
Lubricant	Water	Water	Water	Blue^	Blue^	Blue^	Blue^
Time (min)	0:45	0:45	1:30	4:00	4:00	4:00	3:00
Force (N)	15	15	15	15	15	10	10
Plate (RPM)	300	300	300	150	150	150	130
Head (RPM)	150	150	150	130	130	130	110
Rotation	Co	Co	Co	Counter	Counter	Counter	Counter

Table 11: Polishing parameters

*Propriety polishing cloths; ~Propriety alcohol based diamond suspension; `Alcohol based diamond suspension; ^Propriety alcohol-based lubricant;